produced larger amounts of IFN-γ (40). Thus, non–T cells, such as NK cells, in the intestine might be important for intestinal inflammation as well as T cells via IL-23/IFN-γ axis.

As described above, it has become evident that abnormal intestinal macrophages may contribute to intestinal inflammation in patients with CD via IL-23/IFN-γ axis. However, how this abnormal differentiation of macrophages occurs remains unknown. Alternatively, in the normal intestine of humans, intestinal macrophages lack the expression of the innate-immune receptor CD14; therefore, intestinal macrophages do not induce inflammatory responses against commensals. A previous study demonstrated that the downregulation of CD14 expression is dependent on TGF-β produced by intestinal stromal cells (11). The present study indicated that proinflammatory cytokines, such as IFN-γ, induced abnormal differentiation of intestinal macrophage with IL-23–producing intestinal macrophage phenotypes. Because IFN-γ suppresses the TGF-β/Smad signaling (41), IFN-γ was involved not only in IL-23 production but also in the retention of CD14 antigen expression on such abnormal macrophages. On the other hand, IL-6 production was enhanced both in UC- and CD-CM–induced macrophages. These results suggest that some common inflammatory mediators, which are present in both UC and CD LPMC-CMs, were responsible for the enhancement of IL-6 production by macrophages, while inflammatory mediators that predominate in CD, such as IFN-γ, might contribute to the enhanced IL-23 and IL-12/IL-23p40 production. In contrast to the cytokine producing ability, there were no significant differences in surface markers among macrophages induced by normal-, UC- and CD-CMs (Figure 6B). However, at present, we have only examined the expression of CD14, CD33, CD209, and CD206 and did not examine the other markers. Therefore, the possibility exists that the expression of other markers is different between these macrophages induced by normal-, UC-, and CD-CM. Further studies are required to clarify the markers that distinguish the $CD14^+$ macrophages with the IL-23–hyperproducing ability. Moreover, we also demonstrated that monocytes in CD patients were distinct from those in normal controls and were more susceptible to CD-CM–induced abnormal macrophage differentiation, and the levels of IL-23 and IL-12p40 production by CD monocyte–derived abnormal macrophages were markedly higher than those in normal monocyte–derived abnormal macrophages. This implies a possibility that monocytes from CD patients exhibit high susceptibility to IFN-γ activations of the IL-23–hyperproducing phenotype. In contrast, although $CD14^+$ intestinal macrophages in patients with CD revealed enhanced production of not only IL-23 but also TNF-α compared with those in normal and patients with UC, CD-CM did not elicit any effect on TNF-α production by macrophages derived from healthy monocytes (Figure 6D). At present we do not know whether CD-CM affects not only IL-23 but also TNF-α production on CD monocyte–derived macrophages. A number of unresolved issues still remain; however, these results indicate the possibility that some kind of intrinsic abnormality is imprinted in the monocyte of CD patients, which leads to enhanced TNF-α production by intestinal macrophages independent from the inflammatory microenvironment.

Our present study identifies what we believe to be unique macrophages that may play a central role in Th1- or Th17/Th1-skewed intestinal inflammation in human CD via IL-23 and TNF-α. Moreover, such inflammatory skewed intestinal microenvironments triggered further abnormal macrophage differentiation with IL-23 hyperproduction, which is dependent on IFN-γ (Supplemental Figure 6). Collectively, this IL-23/IFN-γ–positive feedback loop induced by abnormal intestinal macrophages contributes to the pathogenesis of chronic intestinal inflammation in patients with CD.

Methods

Tissue samples. Normal intestinal mucosa was obtained from macroscopically and microscopically unaffected areas of patients with colon cancer. Intestinal mucosa was also obtained from surgically resected specimens from patients with UC or CD, diagnosed on the basis of clinical, radiographic, endoscopic, and histological findings according to established criteria. In all samples from patients with CD or UC, the degree of inflammation was histologically moderate to severe. All experiments were approved by the institutional review board of Keio University School of Medicine and written informed consent was obtained from all patients.

Histological analysis. Tissue sections were treated according to well-established methods. Intestinal specimens were fixed with 4% paraformaldehyde (Wako Pure Chemical Industries) and embedded in paraffin. For immunohistochemical staining, deparaffinized sections were heated at 100°C for 20 minutes in 10 mM sodium citrate buffer (pH 6.0) in a microwave oven. Sections were treated with 3% hydrogen peroxide (H_2O_2) (Wake Pure Chemical Industries) in 100% methanol and then incubated with normal rabbit serum (Nichirei Biosciences) for 15 minutes at room temperature to block nonspecific reactions. Thereafter, they were incubated with mouse anti-human CD14 Ab (Zymed Laboratories) at 4°C overnight. After washing with PBS, the sections were incubated with Alexa Fluor 488–conjugated secondary antibody (Molecular Probes). In the case of double labeling, slides were boiled for 15 minutes and treated in 3% H_2O_2/methanol for 10 minutes after completion of the first staining. This procedure completely blocked the antigenicity of the first primary and secondary antibody. Then, the same staining procedures were performed with the second primary antibody, mouse anti-human CD68 Ab (Dako Cytomation), and Alexa Fluor 568–conjugated secondary antibody. Sections were then washed in PBS, incubated with DAPI to stain nuclei, and examined and photographed using fluorescence microscopy (Nikon Eclipse 80i). In the case of DAB staining, Histofine anti-mouse Simplestain Max-PO (Nichirei) was used as the secondary antibody. Bound antibody was visualized with 3-3′-diaaminobenzidine (DAB; Nichirei), and sections were counterstained with hematoxylin.

Preparation of LPMCs. LPMCs were isolated from intestinal specimens using modifications of previously described techniques (17). Briefly, dissected mucosa was incubated in calcium and magnesium-free HBSS (Sigma-Aldrich) containing 2.5% heat-inactivated fetal bovine serum (BioSource) and 1 mM dithiothreitol (Sigma-Aldrich) to remove mucus. The mucosa was then incubated twice in HBSS containing 1 mM EDTA (Sigma-Aldrich) for 45 minutes at 37°C. Tissues were collected and incubated in HBSS containing 1 mg/ml collagenase type 3 and 0.1 mg/ml DNase I (Worthington Biochemical) for 60 minutes at 37°C. The fraction was pelleted and resuspended in a 40% Percoll solution (Amersham Biosciences), then layered on 60% Percoll before centrifugation at 700 *g* for 20 minutes at room temperature. Viable LPMCs were recovered from the 40%–60% layer interface.

Isolation of PB monocytes or LP $CD14^+CD33^+$ or $CD14^-CD33^+$ macrophages. Peripheral $CD14^+$ monocytes were isolated from PBMCs using $CD14^+$ MACS (Miltenyi Biotec) according to the manufacturer's instructions. The percentage of monocytes isolated using this method was evaluated by flow cytometry and was routinely more than 98%. LP $CD14^+CD33^+$ macrophages were isolated from LPMCs using EasySep Human $CD14^+$ (StemCell Technologies Inc.). $CD14^-CD33^+$ macrophages were isolated from LPMCs using MACS and EasySep (as $CD14^-CD3^-CD56^-CD33^+$ cells). The percentage of each subset of cells isolated using this method was evaluated by flow cytometry and was routinely more than 95%.

Flow cytometric analysis. Cell-surface fluorescence intensity was assessed using a FACSCalibur analyzer and analyzed using CellQuest software (BD Biosciences) or FlowJo (TreeStar). Dead cells were excluded with propidium iodide staining. Monoclonal antibodies for CD14, CD33, CD13, CD16, CD32, CD64, CD71, CD123, CD80, CD86, CD1a, CD83, CD40, CD206, CD209, HLA-DR, CCR1, CCR2, CCR7, CCR9, CXCR1, CXCR2, CXCR4, CD68, CD208, CD36, TREM-1, PD-L1, CD70, and CD103 were purchased from BD Biosciences. Abs for CD205, TLR2, TLR4, and PD-L2 were from eBioscience. Abs for CCR4, CCR5, and CCR6 were from R&D Systems. The CD1c Ab was from Ancell. CX_3CR1 Ab was from MBL.

Commensal bacteria heat-killed antigens. A gram-negative nonpathogenic commensal strain of *E. coli* (catalog no. 25922; ATCC) was cultured in Luria-Bertani (LB) medium, and a gram-positive commensal strain of *E. faecalis* (catalog no. 29212; ATCC) was cultured in brain-heart infusion (BHI) medium. Bacteria were harvested and washed twice with ice-cold PBS. Then, bacterial suspensions were heated at 80°C for 30 minutes, washed, resuspended in PBS, and stored at -80°C. Complete killing was confirmed by a 72-hour incubation at 37°C on plate medium.

Stimulation of macrophages by commensal bacteria antigens. Isolated macrophages were seeded on 96-well tissue culture plates (1×10^6 cells/ml) in RPMI 1640 medium supplemented with 10% FBS, antibiotics (100 units/ml penicillin and 100 μg/ml streptomycin), 10 mM HEPES, and 50 μM 2-mercaptoethanol and stimulated with heat-killed bacteria (1×10^8 CFU/ml) for 24 hours. Culture supernatants and total RNAs were collected and then stored at -80°C until the cytokine assay.

Stimulation of LPMCs. Isolated whole LPMCs were seeded on 96-well tissue culture plates (1×10^6 cells/ml) and stimulated with 20 ng/ml recombinant human IL-23, TNF-α, and IL-6 (all from R&D Systems) or heat-killed bacteria (1×10^8 CFU/ml) with or without 1 μg/ml anti-human IL-12/IL-23p40 Ab (eBiosciences), anti-human TNF-α Ab (R&D Systems), or the same amount of mouse IgG_1 (R&D Systems) for 24 hours. For measurement of secreted cytokines, culture supernatants were collected and stored at -80°C until the cytokine assay.

Preparation of LPMC-CM. Isolated LPMCs from the intestine of normal control subjects or the inflamed mucosa of IBD patients were cultured for 60 hours without any stimulation. Culture supernatants were collected, passed through a 0.22-μm filter, and then stored at -80°C until used.

In vitro macrophage differentiation. PB $CD14^+$ monocytes were isolated from healthy donors or CD patients. $CD14^+$ monocytes were cultured with 50 ng/ml recombinant human M-CSF (R&D Systems) for 6 days to obtain macrophages. Differentiated macrophages were harvested, washed to remove residual cytokines, and then plated on 96-well tissue culture plates (5×10^5 cells/ml) in RPMI 1640 medium supplemented with 10% FBS, antibiotics (100 units/ml penicillin and 100 μg/ml streptomycin), 10 mM HEPES, 50 μM 2-mercaptoethanol, and 50 ng/ml M-CSF. After a 2-hour preincubation, macrophages were stimulated with bacterial antigens. In some experiments, LPMC-CM (10% of final volume), recombinant IFN-γ (100 ng/ml), anti–IFN-γ Ab (1 μg/ml), and anti–IFN-γ receptor 1 Ab (10 μg/ml) were added during the macrophage differentiation process. For the differentiation experiments, mouse IgG_1 (for IFN-γ receptor 1 Ab) and mouse IgG_{2A} (for IFN-γ Ab) were used at the same concentrations as controls.

Quantitative real-time RT-PCR analysis. Total RNA was extracted using an RNeasy Micro kit (QIAGEN), and cDNA was synthesized using a Quantitect RT kit (QIAGEN) according to the manufacturer's instructions. Quantitative real-time RT-PCR was performed using a TaqMan Universal PCR Master Mix (Applied Biosystems) and on-demand gene-specific primers, assessed using the DNA Engine Opticon 2 System (Bio-Rad), and analyzed with Opticon monitor software (MJ Research). The primers were as follows: *IL12p35* (Hs00168405), *IL12p40* (Hs00233688), *IL23p19* (Hs00372324), *IL27p28* (Hs00377366), *Tgfb1* (Hs00171257), *IFNG* (Hs00174143), *IL17* (Hs00174383), *IL22* (Hs00220924), *CCL20* (Hs00171125), *ACTB* (Hs99999903). All primers were purchased from Applied Biosystems. Relative quantification was achieved by normalizing to the values of the *Actb* gene.

Cytokine assay. The following kits were used for cytokine measurements and tests were performed according to the manufacturer's instructions: human IL-12p40 ELISA (BD Pharmingen), human IL-23 ELISA (BenderMed Systems), human IL-17 ELISA (R&D Systems), human TGF-β1 ELISA (R&D Systems), and human inflammation or Th1/Th2-II cytometric beads array (CBA) kit (BD Pharmingen).

Statistics. Statistical analysis was performed using GraphPad Prism software version 4.0 (GraphPad Software Inc.). Differences of $P < 0.05$ were considered to be significant. All data are expressed as mean ± SEM.

Acknowledgments

We thank Y. Iwao, H. Ogata, and T. Yajima (Keio University) for providing human materials and for helpful discussions and critical comments. We thank T. Nakai, K. Arai, and Y. Wada (Keio University) for technical assistance. This work was supported in part by Grant-in Aid for Scientific Research from the Ministry of Education, Culture, Sports, Science, and Technology, Japan Society for the Promotion of Science, and Keio University Medical Fund.

Received for publication November 28, 2007, and accepted in revised form April 9, 2008.

Address correspondence to: T. Hibi, Division of Gastroenterology and Hepatology, Department of Internal Medicine, Keio University School of Medicine, 35 Shinanomachi, Shinjuku-ku, Tokyo 160-8582, Japan. Phone: 81-3-3357-6156; Fax: 81-3-3357-6156; E-mail: thibi@sc.itc.keio.ac.jp.

1. Xavier, R.J., and Podolsky, D.K. 2007. Unravelling the pathogenesis of inflammatory bowel disease. *Nature.* **448**:427-434.
2. Hibi, T., and Ogata, H. 2006. Novel pathophysiological concepts of inflammatory bowel disease. *J. Gastroenterol.* **41**:10-16.
3. Fuss, I.J., et al. 1996. Disparate CD4+ lamina propria (LP) lymphokine secretion profiles in inflammatory bowel disease. Crohn's disease LP cells manifest increased secretion of IFN-gamma, whereas ulcerative colitis LP cells manifest increased secretion of IL-5. *J. Immunol.* **157**:1261-1270.
4. Matsuoka, K., et al. 2004. T-bet upregulation and subsequent interleukin 12 stimulation are essential for induction of Th1 mediated immunopathology in Crohn's disease. *Gut.* **53**:1303-1308.
5. Sartor, R.B. 2006. Mechanisms of disease: pathogenesis of Crohn's disease and ulcerative colitis. *Nat. Clin. Pract. Gastroenterol. Hepatol.* **3**:390-407.
6. Gordon, S., and Taylor, P.R. 2005. Monocyte and macrophage heterogeneity. *Nat. Rev. Immunol.* **5**:953-964.
7. Mantovani, A., et al. 2004. The chemokine system in diverse forms of macrophage activation and polarization. *Trends Immunol.* **25**:677-686.
8. Mosser, D.M. 2003. The many faces of macrophage activation. *J. Leukoc. Biol.* **73**:209-212.
9. Rogler, G., et al. 1998. Isolation and phenotypic characterization of colonic macrophages. *Clin. Exp. Immunol.* **112**:205-215.
10. Smith, P.D., et al. 2001. Intestinal macrophages lack CD14 and CD89 and consequently are down-regulated for LPS- and IgA-mediated activities. *J. Immunol.* **167**:2651-2656.
11. Smythies, L.E., et al. 2005. Human intestinal macrophages display profound inflammatory anergy despite avid phagocytic and bacteriocidal activity. *J. Clin. Invest.* **115**:66-75.
12. Denning, T.L., Wang, Y.C., Patel, S.R., Williams, I.R., and Pulendran, B. 2007. Lamina propria macrophages and dendritic cells differentially induce regulatory and interleukin 17-producing T cell responses. *Nat. Immunol.* **8**:1086-1094.
13. Schenk, M., and Mueller, C. 2007. Adaptations of intestinal macrophages to an antigen-rich environment. *Semin. Immunol.* **19**:84-93.
14. Kobayashi, M., et al. 2003. Toll-like receptor-dependent production of IL-12p40 causes chronic enterocolitis in myeloid cell-specific Stat3-deficient mice. *J. Clin. Invest.* **111**:1297-1308.
15. Hirotani, T., et al. 2005. The nuclear IkappaB protein IkappaBNS selectively inhibits lipopolysaccharide-induced IL-6 production in macrophages of the colonic lamina propria. *J. Immunol.*

174:3650–3657.
16. Kanai, T., et al. 2000. Interleukin 18 is a potent proliferative factor for intestinal mucosal lymphocytes in Crohn's disease. *Gastroenterology.* **119**:1514–1523.
17. Kanai, T., et al. 2001. Macrophage-derived IL-18-mediated intestinal inflammation in the murine model of Crohn's disease. *Gastroenterology.* **121**:875–888.
18. Fuss, I.J., et al. 2006. Both IL-12p70 and IL-23 are synthesized during active Crohn's disease and are down-regulated by treatment with anti-IL-12 p40 monoclonal antibody. *Inflamm. Bowel Dis.* **12**:9–15.
19. Schenk, M., Bouchon, A., Seibold, F., and Mueller, C. 2007. TREM-1–expressing intestinal macrophages crucially amplify chronic inflammation in experimental colitis and inflammatory bowel diseases. *J. Clin. Invest.* **117**:3097–3106.
20. Kamada, N., et al. 2005. Abnormally differentiated subsets of intestinal macrophage play a key role in Th1-dominant chronic colitis through excess production of IL-12 and IL-23 in response to bacteria. *J. Immunol.* **175**:6900–6908.
21. Grimm, M.C., Pavli, P., Van de Pol, E., and Doe, W.F. 1995. Evidence for a CD14+ population of monocytes in inflammatory bowel disease mucosa – implications for pathogenesis. *Clin. Exp. Immunol.* **100**:291–297.
22. Rugtveit, J., et al. 1997. Cytokine profiles differ in newly recruited and resident subsets of mucosal macrophages from inflammatory bowel disease. *Gastroenterology.* **112**:1493–1505.
23. Geissmann, F., Jung, S., and Littman, D.R. 2003. Blood monocytes consist of two principal subsets with distinct migratory properties. *Immunity.* **19**:71–82.
24. Mizoguchi, A., et al. 2007. Dependence of intestinal granuloma formation on unique myeloid DC-like cells. *J. Clin. Invest.* **117**:605–615.
25. Kim, S.C., et al. 2005. Variable phenotypes of enterocolitis in interleukin 10-deficient mice monoassociated with two different commensal bacteria. *Gastroenterology.* **128**:891–906.
26. van Beelen, A.J., et al. 2007. Stimulation of the intracellular bacterial sensor NOD2 programs dendritic cells to promote interleukin-17 production in human memory T cells. *Immunity.* **27**:660–669.
27. Cua, D.J., et al. 2003. Interleukin-23 rather than interleukin-12 is the critical cytokine for autoimmune inflammation of the brain. *Nature.* **421**:744–748.
28. Murphy, C.A., et al. 2003. Divergent pro- and antiinflammatory roles for IL-23 and IL-12 in joint autoimmune inflammation. *J. Exp. Med.* **198**:1951–1957.
29. Langrish, C.L., et al. 2005. IL-23 drives a pathogenic T cell population that induces autoimmune inflammation. *J. Exp. Med.* **201**:233–240.
30. Vaknin-Dembinsky, A., Balashov, K., and Weiner, H.L. 2006. IL-23 is increased in dendritic cells in multiple sclerosis and down-regulation of IL-23 by antisense oligos increases dendritic cell IL-10 production. *J. Immunol.* **176**:7768–7774.
31. Neurath, M.F. 2007. IL-23: a master regulator in Crohn disease. *Nat. Med.* **13**:26–28.
32. Yen, D., et al. 2006. IL-23 is essential for T cell-mediated colitis and promotes inflammation via IL-17 and IL-6. *J. Clin. Invest.* **116**:1310–1316.
33. Duerr, R.H., et al. 2006. A genome-wide association study identifies IL23R as an inflammatory bowel disease gene. *Science.* **314**:1461–1463.
34. Uhlig, H.H., et al. 2006. Differential activity of IL-12 and IL-23 in mucosal and systemic innate immune pathology. *Immunity.* **25**:309–318.
35. Annunziato, F., et al. 2007. Phenotypic and functional features of human Th17 cells. *J. Exp. Med.* **204**:1849–1861.
36. Powrie, F., et al. 1994. Inhibition of Th1 responses prevents inflammatory bowel disease in scid mice reconstituted with CD45RBhi CD4+ T cells. *Immunity.* **1**:553–562.
37. Kullberg, M.C., et al. 1998. Helicobacter hepaticus triggers colitis in specific-pathogen-free interleukin-10 (IL-10)-deficient mice through an IL-12- and gamma interferon-dependent mechanism. *Infect. Immun.* **66**:5157–5166.
38. Hue, S., et al. 2006. Interleukin-23 drives innate and T cell-mediated intestinal inflammation. *J. Exp. Med.* **203**:2473–2483.
39. Kullberg, M.C., et al. 2006. IL-23 plays a key role in Helicobacter hepaticus-induced T cell-dependent colitis. *J. Exp. Med.* **203**:2485–2494.
40. Chinen, H., et al. 2007. Lamina propria c-kit (+) immune precursors reside in human adult intestine and differentiate into natural killer cells. *Gastroenterology.* **133**:559–573.
41. Ulloa, L., Doody, J., and Massague, J. 1999. Inhibition of transforming growth factor-beta/SMAD signalling by the interferon-gamma/STAT pathway. *Nature.* **397**:710–713.

Exacerbating Role of γδ T Cells in Chronic Colitis of T-Cell Receptor α Mutant Mice

MASANOBU NANNO,[*] YASUYOSHI KANARI,[‡] TOMOAKI NAITO,[§,‖] NAGAMU INOUE,[¶] TADAKAZU HISAMATSU,[¶] HIROSHI CHINEN,[¶] KEN SUGIMOTO,[#,**] YASUYO SHIMOMURA,[#,**] HIDEO YAMAGISHI,[‡] TETSUO SHIOHARA,[‡‡] SATOSHI UEHA,[§§] KOUJI MATSUSHIMA,[§§] MAKOTO SUEMATSU,[‖] ATSUSHI MIZOGUCHI,[#,**] TOSHIFUMI HIBI,[¶] ATUL K. BHAN,[#,**] and HIROMICHI ISHIKAWA[§]

[*]*Yakult Central Institute for Microbiological Research, Tokyo;* [‡]*Department of Biophysics, Graduate School of Science, Kyoto University, Kyoto;* [§]*Department of Microbiology and Immunology, Keio University School of Medicine, Tokyo;* [‖]*Department of Biochemistry and Integrative Medical Biology, Keio University School of Medicine, Tokyo;* [¶]*Department of Internal Medicine, Keio University School of Medicine, Tokyo, Japan;* [#]*Center for the Study of Inflammatory Bowel Disease, Massachusetts General Hospital, Boston;* [**]*Department of Pathology, Massachusetts General Hospital, Boston, Massachusetts;* [‡‡]*Department of Dermatology, Kyorin University School of Medicine, Tokyo, Japan; and* [§§]*Department of Molecular Preventive Medicine, Graduate School of Medicine, University of Tokyo, Tokyo, Japan*

Background & Aims: **T-cell receptor (TCR) γδ T cells are an important component of the mucosal immune system and regulate intestinal epithelial homeostasis. Interestingly, there is a significant increase in γδ T cells in the inflamed mucosa of patients with ulcerative colitis (UC). However, the role of γδ T cells in chronic colitis has not been fully identified.** ***Methods:*** **TCRα-deficient mice, which spontaneously develop chronic colitis with many features of human UC including an increase in γδ T-cell population, represent an excellent model to investigate the role of γδ T cells in UC-like colitis. To identify the role of γδ T cells in this colitis, we herein have generated TCRγ-deficient mice through deletion of all TCR Cγ genes (Cγ1, Cγ2, Cγ3, and Cγ4) using the Cre/*loxP* site-specific recombination system and subsequently crossing these mice with TCRα-deficient mice.** ***Results:*** **An increase in colonic γδ T cells was associated with the development of human UC as well as UC-like disease seen in TCRα-deficient mice. Interestingly, the newly established TCRα$^{-/-}$ × TCRγ$^{-/-}$ double mutant mice developed significantly less severe colitis as compared with TCRα-deficient mice. The suppression of colitis in TCRα$^{-/-}$ × TCRγ$^{-/-}$ double mutant mice was associated with a significant reduction of proinflammatory cytokine and chemokine productions and a decrease in neutrophil infiltration.** ***Conclusions:*** **γδ T cells are involved in the exacerbation of UC-like chronic disease. Therefore, γδ T cells may represent a promising therapeutic target for the treatment of human UC.**

T cell receptor (TCR) γδ T cells are an evolutionary conserved T-cell subset with characteristic properties.[1] TCRγδ-bearing murine dendritic epidermal T cells are involved in the regulation of epidermal integrity and promote wound repair of the skin,[2] whereas intestinal intraepithelial γδ T cells (γδ-IEL) regulate intestinal epithelial homeostasis.[3,4] Recent evidence suggests that γδ T cells are also important in immune surveillance of the epithelium by providing a first line of defense against infectious pathogens attacking the surfaces of the body and in the regulation of linking of innate and acquired immunity.[1,5] Furthermore, γδ T cells appear to down-regulate αβ T cell-driven robust immune responses that often result in severe immunopathology.[1]

The incidence of inflammatory bowel diseases (IBD), namely ulcerative colitis (UC) and Crohn's disease (CD), has increased markedly in recent years. The factors including genetic predisposition, environmental conditions, and aberrant immune response driven by normal intestinal flora are vital for the development and persistence of the inflammatory process.[6,7] In the present study, we aimed at elucidating the role of γδ T cells in the pathogenesis of IBD because there is growing evidence supporting that γδ T cells play an active multifaceted immunoregulatory role in the coordinated innate and acquired immune responses that maintain the integrity of epithelial tissues[1,2,4,5,8] and an increase in γδ T cells in the diseased mucosa has been documented in UC patients.[9,10] In acute colitis induced by administration of either 2,4,6-trinitrobenzene sulfonic acid[11,12] or dextran sulfate sodium,[13,14] a protective role of γδ T cells has been demonstrated. However, the role of γδ T cells in chronic intestinal inflammation resembling UC has not yet been investigated. TCRα$^{-/-}$ (α$^{-/-}$) mice spontaneously develop chronic colitis with several features of human UC including a significant increase in γδ T cells.[15] To illuminate the role of γδ T cells in the pathogenesis of UC-like colitis in α$^{-/-}$ mice, we generated TCRγ$^{-/-}$

Abbreviations used in this paper: α$^{-/-}$, TCRα$^{-/-}$; ARP, anorectal prolapse; γ$^{-/-}$, TCRγ$^{-/-}$; γδ T cells, TCR γδ T cells; IBD, inflammatory bowel disease; IEL, intestinal intraepithelial T lymphocytes; LP, lamina propria; TCR, T-cell receptor; UC, ulcerative colitis.

0016-5085/08/$34.00
doi:10.1053/j.gastro.2007.11.056

($\gamma^{-/-}$) mice and examined the severity of colitis in $\alpha^{-/-}$ mice that are genetically engineered to lack γδ T cells.

Materials and Methods

Mice

We newly generated $\gamma^{-/-}$ mice and crossed with $\alpha^{-/-}$ mice[16] to develop double mutant ($\alpha^{-/-} \times \gamma^{-/-}$) mice. The generations of these mice are described in Supplementary Materials (see Supplemental Materials online at www.gastrojournal.org). All mice used were of C57BL/6 (B6) background. The mice were maintained under specific pathogen-free conditions, and all animal procedures described in this study were performed in accordance with the guidelines for animal experiments of Keio University School of Medicine, Yakult Central Institute for Microbiological Research, Kinki University School of Medicine, and Massachusetts General Hospital.

Flow Cytometry and Immunohistochemical Procedures

Methods for isolation of intestinal intraepithelial T cells (IEL) from mouse small intestines and lamina propria (LP) cells from mouse and human large intestines are described in Supplementary Materials. Procedures of cell staining for flow cytometric and immunohistochemical analyses are also described in Supplementary Materials (see Supplemental Materials online at www.gastrojournal.org).

Histologic Evaluation of Colitis

The disease score of colitis (0–10) was estimated in a blind fashion using previously described criteria, namely, a combination of both gross and histologic findings.[17] The gross score was rated as 0, presence of normal beaded appearance; 1, absence of beaded appearance of colon; 2, focally thickened colon; and 3, marked thickness of entire colon. The histologic score was based on the extent of intestinal wall thickening (0–3), inflammatory cell infiltration into LP (0–3), and presence (0 or 1) of ulceration.

Real-Time Reverse-Transcription Polymerase Chain Reaction Analysis

Total RNA was extracted from half of the frozen colonic tissue obtained from each one of wild-type (WT), $\gamma^{-/-}$, $\alpha^{-/-}$, and $\alpha\gamma^{-/-}$ littermate mice, and complementary DNA (cDNA) was prepared. Quantitative real-time reverse-transcription polymerase chain reaction (RT-PCR) was conducted to assess the expression level of TNF-α, IL-1β, IL-6, TGF-β, IFN-γ, IL-7, IL-10, IL-12, KC, MIP-2, GCP-2, MCP-1, MIP-1α, MIP-1β, and HPRT genes using TaqMan probes (Applied Biosystems, Foster City, CA). The relative expression level of genes of interest was normalized to the HPRT gene expression. The detailed procedures are described in Supplementary Materials (see Supplemental Materials online at www.gastrojournal.org).

Measurement of Cytokines and Chemokines by Enzyme-Linked Immunosorbent Assay

Proteins were extracted from the above-described half of the frozen colonic tissue obtained from each one of WT, $\gamma^{-/-}$, $\alpha^{-/-}$, and $\alpha\gamma^{-/-}$ littermate mice. In brief, frozen colonic tissue was homogenized with a sonicator (Ultrasonic Disruptor UD-201, TOMY, Tokyo, Japan) in 5 mL lysis buffer (50 mmol/L Tris-HCl, pH 7.4, 150 mmol/L NaCl, 1% NP-40, 1 mmol/L dithiothreitol, 1 mmol/L EDTA, 1 mmol/L NaF, 1 mmol/L sodium orthovanadate, and complete, Mini EDTA-free proteinase inhibitor [Roche Applied Science, Mannheim, Germany]), the homogenate was clarified by centrifugation at 14,000 rpm for 10 minutes, and the supernatant was subjected to OptEIA ELISA (BD Biosciences, San Diego, CA) for detection of tumor necrosis factor (TNF)-α, interleukin (IL)-1β, and IL-6 and to DuoSet ELISA (R&D Systems, Minneapolis, MN) for detection of transforming growth factor (TGF)-β, interferon (IFN)-γ, keratinocyte-derived chemokine (KC), macrophage inflammatory protein (MIP)-2 and granulocyte chemotactic protein (GCP)-2. Levels in the supernatants were standardized to the total amount of protein in the same supernatants assessed by RC DC Protein Assay (Bio-Rad Laboratories, Hercules, CA).

Chemotaxis Assay

The assays were performed using the ChemoTx 96-well plate No. 101-3 (NeuroProbe, Gaithersburg, MD). Briefly, bone marrow cells collected from femurs, tibias, and humerus of WT mice were recovered by centrifugation at the interphase of 44% and 70% Percoll solutions. Subsequently, 2.5×10^5 bone marrow cells were loaded onto the membrane plate and placed on a flat-bottomed, 96-well microtiter plate containing the colon extracts (0.7 mg protein/mL) from WT, $\alpha^{-/-}$, and $\alpha\gamma^{-/-}$ mice in addition to serially diluted MIP-2 and MCP-1 (R&D Systems). To identify the neutrophils and monocytes, bone marrow cells were labeled with fluorescent dye conjugated monoclonal antibodies (mAb) to Mac-1 and Ly-6C before the assay. After incubation at 37°C for 2 hours, the number of Mac-1$^+$Ly-6C^{low} neutrophils[18] and Mac-1$^+$Ly-6C^{high} monocytes[18] that migrated into the lower wells was determined by a flow cytometry.

Cell Transfer

γδ T cells were purified from the mesenteric lymph nodes (MLNs) and colon of $\alpha^{-/-}$ mice through MACS system, and 2×10^6 purified cells were intravenously transferred twice into $\alpha\gamma^{-/-}$ mice (n = 16) at 4 and 5 months of age. As control group, phosphate-buffered saline (PBS) was intravenously administrated into $\alpha\gamma^{-/-}$ mice (n = 15). The recipient mice were then killed at 6 months of age.

Statistical Analysis

The statistical difference was determined by 2-sided Student *t* test. For the statistical analysis of cell infiltration into the large intestine, 2-sided Mann-Whitney *U* test was used. Difference with $P < .05$ was considered significant.

Results

Generation of TCRγ-Deficient Mice

To begin with, we initially confirmed that γδ T cells were increased in the lymphoid cells isolated from the inflamed colonic mucosa of UC patients as compared with those from the unaffected colonic mucosa of patients with colon cancer (Figure 1*A* and *B*) and also in the lymphoid cells isolated from the inflamed colonic LP of $\alpha^{-/-}$ mice as compared with those from normal colonic LP of age-matched WT littermate mice (Figure 1C and *D*).

Precise appreciation of the role of γδ T cells in pathogenesis of colitis in $\alpha^{-/-}$ mice requires the generation of $\alpha^{-/-}$ mice deficient in γδ T cells. However, the previously generated TCR$\delta^{-/-}$ ($\delta^{-/-}$) mice[19] lacking γδ T cells could not be used for this purpose because of the genomic localization of TCRδ coding segments within the *V* and *J* segments of TCRα gene.[20] To overcome this difficulty, we newly generated TCR$\gamma^{-/-}$ mice by disrupting the genes encoding TCR Cγ1, 2, 3, and 4 (CγΔ) using the Cre/*loxP* site-specific recombination system shown in Figure 2. The targeting vector pCγ4ΔNL carrying a *loxP*-flanked *pgk-neo* gene cassette in place of exon 1 of the Cγ4 gene (Figure 2*A*) was introduced into the embryonic stem (ES) clone Vγ6ΔL carrying the allele in which the Vγ6 region was replaced by a single *loxP* site (Figure 2*B*). Transfected cells were cultured in the presence of G418, and G418-resistant recombinant clones showing the joint transmission of Vγ6ΔL and Cγ4ΔNL genes were selected. These ES clones, including the clones carrying both transgenes on the same chromosome, Vγ6ΔL-Cγ4ΔNL (Figure 2C), were injected into B6 blastocysts. The chimeric mice obtained were crossed to the CAG-*cre* transgenic B6 mice to generate the Cγ1-, 2-, 3-, and 4-depleted TCRγ-deficient (CγΔ) allele (Figure 2C) by *cre*-mediated recombination in F_1 mice during embryonic development.

Subsequently, these F_1 mice were intercrossed to produce homozygous ($\gamma^{-/-}$) mice (Figure 2*D*), and these mutant $\gamma^{-/-}$ mice were backcrossed 8 times to B6 mice to obtain $\gamma^{-/-}$ mice carrying the B6 background. WT ($\alpha^{+/-} \times \gamma^{+/-}$), $\gamma^{-/-}$ ($\alpha^{+/-} \times \gamma^{-/-}$), $\alpha^{-/-}$ ($\alpha^{-/-} \times \gamma^{+/-}$), and $\alpha\gamma^{-/-}$ ($\alpha^{-/-} \times \gamma^{-/-}$) littermate F_2 mice were then produced by intercrossing $\alpha^{-/-}$ mice[16] with $\gamma^{-/-}$ mice. Flow cytometric analysis of IEL from the small intestine confirmed that γδ T cells were absent in $\gamma^{-/-}$ and $\alpha\gamma^{-/-}$ mice (Figure 2*E*).

Pathogenic Role of γδ T Cells in UC-Like Colitis

Histologic examination of the colons from 20- to 32-week-old $\alpha^{-/-}$ and $\alpha\gamma^{-/-}$ mice revealed that inflam-

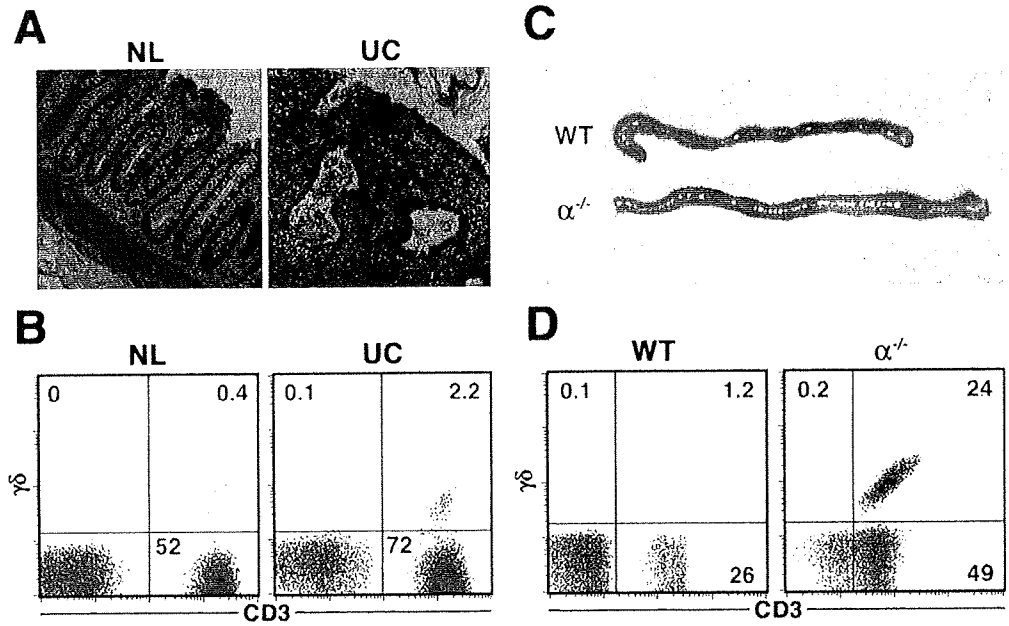

Figure 1. γδ T cells concentrate in the inflamed colonic mucosa of UC patients and colonic LP of $\alpha^{-/-}$ mice suffering from spontaneous chronic colitis. (*A*) A representative colonic tissue section from an ulcerative colitis (*UC*) patient shows a marked infiltration of lymphomyeloid cells, mucosal distortion, crypt abscess, and depletion of goblet cells compared with a normal colonic tissue section (*NL*) (original magnification, ×100). (*B*) A flow cytometry shows increased γδ T-cell population in a diseased colonic LP of UC patient compared with that in a normal colonic LP. This is a representative result of 3 UC patients. (*C*) Large intestines from wild-type (*WT*) mice and $\alpha^{-/-}$ mice suffering from spontaneous chronic colitis are shown. (*D*) A flow cytometry shows increased γδ T-cell population in a diseased colonic LP of $\alpha^{-/-}$ mice compared with that in colonic LP of WT littermate.

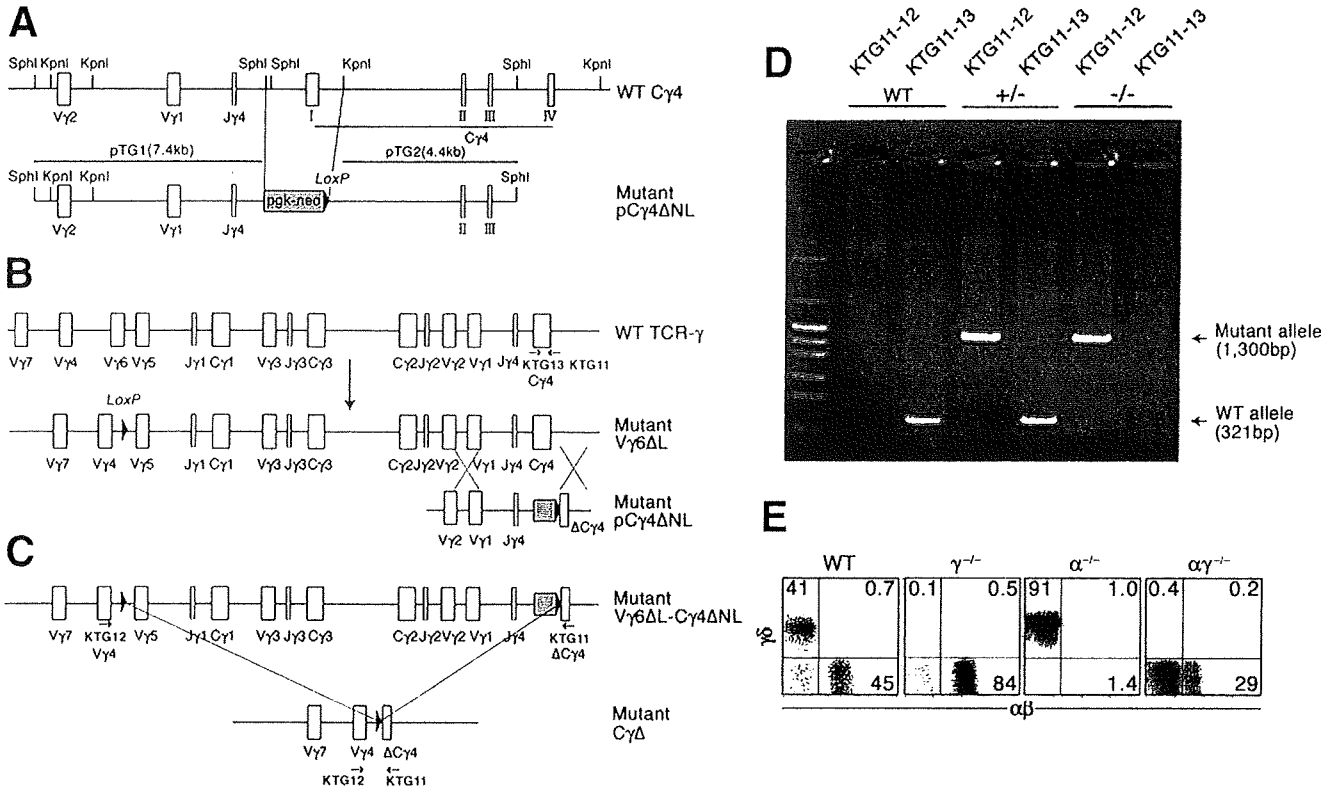

Figure 2. Generation of TCRγ-deficient mice and subsequent production of TCRαγ double mutant mice. (*A*) Schematic representation of WT and mutant (pCγ4ΔNL) genomic Cγ4 loci together with the 3 DNA fragments used to construct the mutant pCγ4ΔNL vector. The resulting targeting vector (pCγ4ΔNL) carrying a *loxP*-flanked *pgk-neo* gene cassette in place of exon 1 of Cγ4 gene used a neomycin resistance gene driven by the *pgk* promoter as positive selection marker is shown. Restriction enzyme sites, *SphI* and *KpnI* (*solid bars*), exon structures, Vγ and Jγ (*open boxes*), and *loxP* site (*solid triangle*) are indicated. (*B*) Schematic representation of the ES clone carrying WT TCRγ gene and mutant Vγ6ΔL ES clone carrying the allele in which the Vγ6 region was replaced by a single *loxP* site and mutant pCγ4ΔNL targeting vector. Exon structures, Vγ and Jγ (*open boxes*) and *loxP* site (*solid triangle*) are indicated. (*C*) Schematic representation of generation of the mutant mice that carry the TCRγ-deficient (CγΔ) allele by Cre-mediated recombination during embryonic development. Exon structures, Vγ and Jγ (*open boxes*), and *loxP* site (*solid triangle*) are indicated. (*D*) The mutant mice that carry the TCRγ-deficient (CγΔ) allele were intercrossed to produce TCR$\gamma^{+/+}$ (WT), TCR$\gamma^{+/-}$ ($\gamma^{+/-}$), and TCR$\gamma^{-/-}$ ($\gamma^{-/-}$) mice, and the corresponding WT and mutant alleles were typed by PCR analysis of tail DNA with each set of primers indicated. (*E*) γδ T cells are absent from the IEL compartment of $\gamma^{-/-}$ and $\alpha\gamma^{-/-}$ mice. $\gamma^{-/-}$ Mice were crossed with $\alpha^{-/-}$ mice to obtain WT ($\alpha^{+/-} \times \gamma^{+/-}$), $\gamma^{-/-}$ ($\alpha^{+/-} \times \gamma^{-/-}$), $\alpha^{-/-}$ ($\alpha^{-/-} \times \gamma^{+/-}$), and $\alpha\gamma^{-/-}$ ($\alpha^{-/-} \times \gamma^{-/-}$) littermate mice.

mation characterized by elongation of crypts was much milder in $\alpha\gamma^{-/-}$ mice as compared with $\alpha^{-/-}$ mice (Figure 3*A*). Although the body weight was comparable between $\alpha\gamma^{-/-}$ and $\alpha^{-/-}$ mice, it was evident that colonic weight was significantly decreased in $\alpha\gamma^{-/-}$ mice as compared with $\alpha^{-/-}$ mice (Figure 3*B*). The disease score characterized by the thickening of colonic mucosa with crypt elongation and inflammatory cell infiltration was also significantly lower in $\alpha\gamma^{-/-}$ mice than that rated in $\alpha^{-/-}$ mice (Figure 3*C*). Although approximately 20% of 20- to 60-week-old $\alpha^{-/-}$ mice displayed anorectal prolapse (ARP), it was not discerned in any of age-matched $\alpha\gamma^{-/-}$ mice (Figure 3*D*). Notably, no difference was observed in the age of onset of colitis and in the incidence of colitis (~80%) among 20- to 32-week-old $\alpha\gamma^{-/-}$ and $\alpha^{-/-}$ mice. In addition, in comparison with administration of PBS (as control), adoptive transfer of γδ T cells that were purified from $\alpha^{-/-}$ mice did not increase the incidence of colitis in the recipient $\alpha\gamma^{-/-}$ mice. However, the transfer of γδ T cells exacerbated the severity of colitis in the recipient $\alpha\gamma^{-/-}$ mice. As shown in Figure 3*E*, more severe inflammatory cell infiltration was observed in the inflamed colon of the recipient $\alpha\gamma^{-/-}$ mice with γδ T-cell transfer as compared with control $\alpha\gamma^{-/-}$ mice. Therefore, it is possible that γδ T cells may be involved in the exacerbation, but not induction, of UC-like colitis.

Decrease in the Colonic Neutrophils and Monocytes in the Absence of γδ T Cells

The above results indicate that the spontaneous colitis in $\alpha^{-/-}$ mice is ameliorated by the absence of γδ T cells in $\alpha\gamma^{-/-}$ mice. With these findings in mind, flow cytometric analysis of colonic LP cells isolated from WT, $\gamma^{-/-}$, $\alpha^{-/-}$, and $\alpha\gamma^{-/-}$ littermate mice at approximately 28 weeks of age was performed, and the representative results of 5 independent experiments are presented in Figure 4*A*. In this experiment, WT, $\gamma^{-/-}$, $\alpha^{-/-}$, and $\alpha\gamma^{-/-}$ littermate mice yielded 5.1×10^5, 6.1

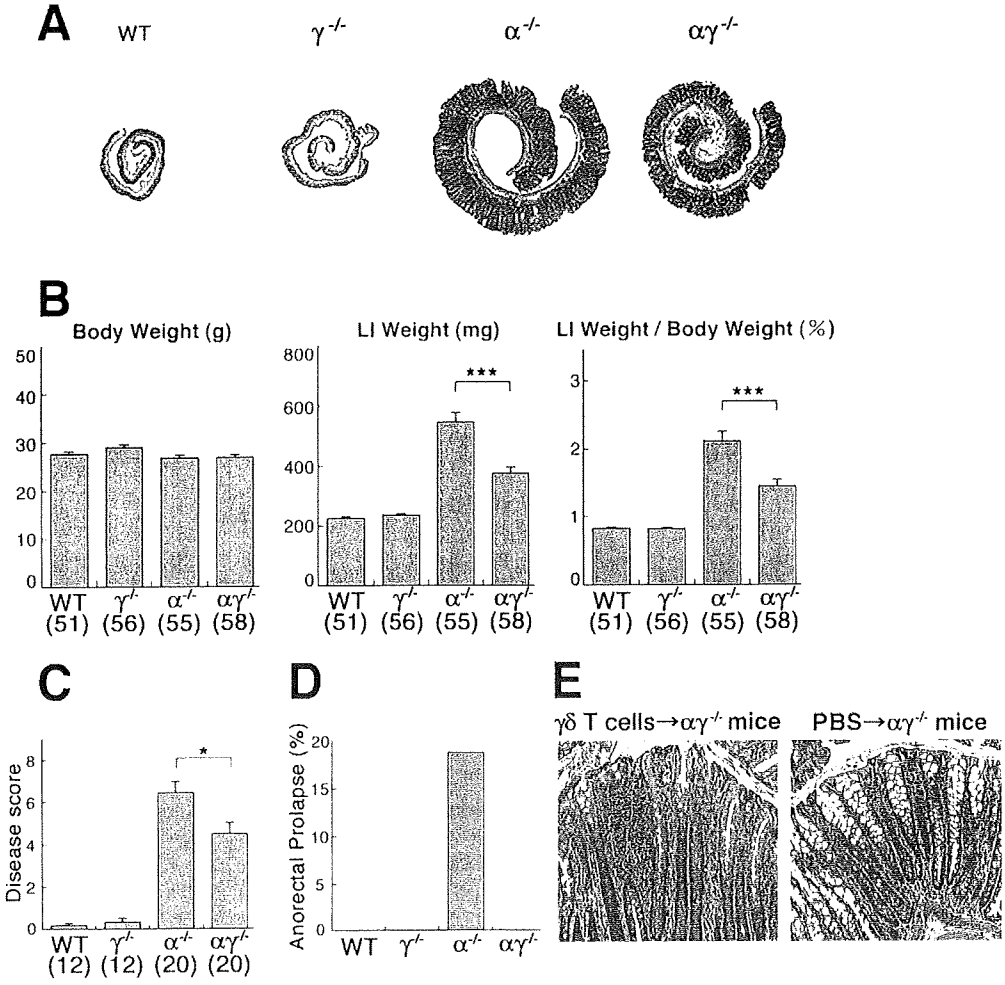

Figure 3. Colonic mucosal inflammation is milder in $\alpha\gamma^{-/-}$ mice lacking γδ T cells than in $\alpha^{-/-}$ mice possessing γδ T cells. (*A*) Representative histologic pictures of colon from WT, $\gamma^{-/-}$, $\alpha^{-/-}$, and $\alpha\gamma^{-/-}$ littermate mice. These mice were maintained in the same cages under specific pathogen-free conditions and examined at 28 weeks of age. (*B*) Body weight, wet weight of large intestine (LI weight), and ratio (%) of LI weight to body weight in WT, $\gamma^{-/-}$, $\alpha^{-/-}$, and $\alpha\gamma^{-/-}$ littermate mice at 20 to 32 weeks of age are shown. Values in parentheses are numbers of mice examined. $^{***}P < .001$. (*C*) Disease scores (0–10) of colitis in 24- to 32-week-old WT, $\gamma^{-/-}$, $\alpha^{-/-}$, and $\alpha\gamma^{-/-}$ mice were assessed. Values in parentheses are numbers of mice examined. $^{*}P < .05$. (*D*) Incidence of ARP in 24- to 60-week-old WT, $\gamma^{-/-}$, $\alpha^{-/-}$, and $\alpha\gamma^{-/-}$ mice. (*E*) The histologic findings (original magnification, ×20) of colon of recipient $\alpha\gamma^{-/-}$ mouse groups that received transfer of γδ T cells (*left panel*) and that received PBS (*right panel*).

× 10^5, 32.3 × 10^5, and 12.0 × 10^5 colonic LP cells, respectively. Based on the absolute numbers of infiltrated cells and the flow cytometry results shown in Figure 4*A*, it was evident that fewer Mac-1$^+$Ly-6G$^-$ cells and Mac-1$^+$Ly-6G$^+$ cells were present in the colonic LP cell population of $\alpha\gamma^{-/-}$ mice as compared with those of $\alpha^{-/-}$ mice. Monocytes express Mac-1 but not Ly-6G, whereas neutrophils express both Mac-1 and Ly-6G.[21] Therefore, our results suggest that, in addition to monocyte infiltration (Figure 4*A*), there is a marked infiltration of neutrophils in the inflamed colonic LP of $\alpha^{-/-}$ mice. We also confirmed our previous finding[15] that a remarkable increase in γδ T cells was observed in the inflamed colonic LP of $\alpha^{-/-}$ mice (Figure 4*A*).

Immunohistochemical examination of inflamed colons from $\alpha^{-/-}$ and $\alpha\gamma^{-/-}$ mice at approximately 28 weeks of age was performed to further confirm flow cytometric results. Consistent with the flow cytometric observations, significantly smaller numbers of Mac-1$^+$ cells and Ly-6G$^+$ cells were observed in the colonic LP of $\alpha\gamma^{-/-}$ mice as compared with those in the colonic LP of $\alpha^{-/-}$ mice (Figure 4*B*).

To investigate whether γδ T cells contribute to the generation of colonic environment for enhancing the migration of neutrophils and monocytes into the inflamed colon, we examined chemotactic activity of colonic extracts from $\alpha^{-/-}$ and $\alpha\gamma^{-/-}$ mice to neutrophils and monocytes (Figure 5*A*). As a result, chemotactic activity to neutrophils of colonic extracts from $\alpha\gamma^{-/-}$ mice was significantly weaker than that from $\alpha^{-/-}$ mice, whereas the chemotactic activities to monocytes of both extracts were almost comparable (Figure 5*B*). The marked infiltration of neutrophils into the inflamed colonic LP of $\alpha^{-/-}$ mice is most likely mediated by some factors, such as MIP-2 (Figure 5*A*), that are enhanced in the presence of γδ T cells.

Taking all of these results together, and in conjunction with our previous findings,[22] colonic γδ T cells of $\alpha^{-/-}$ mice exert aggravating effect on the UC-like colitis by increasing primarily the influx of neutrophils into the inflamed mucosa.

Attenuation of Colonic Proinflammatory Cascades by the Absence of γδ T Cells

In view of the severe colitis, increased infiltration of Mac-1$^+$Ly-6G$^+$ and Mac-1$^+$Ly-6G$^-$ cells, and marked production of neutrophil chemotactic factor(s) in the inflamed colonic LP of $\alpha^{-/-}$ mice, quantitative real-time

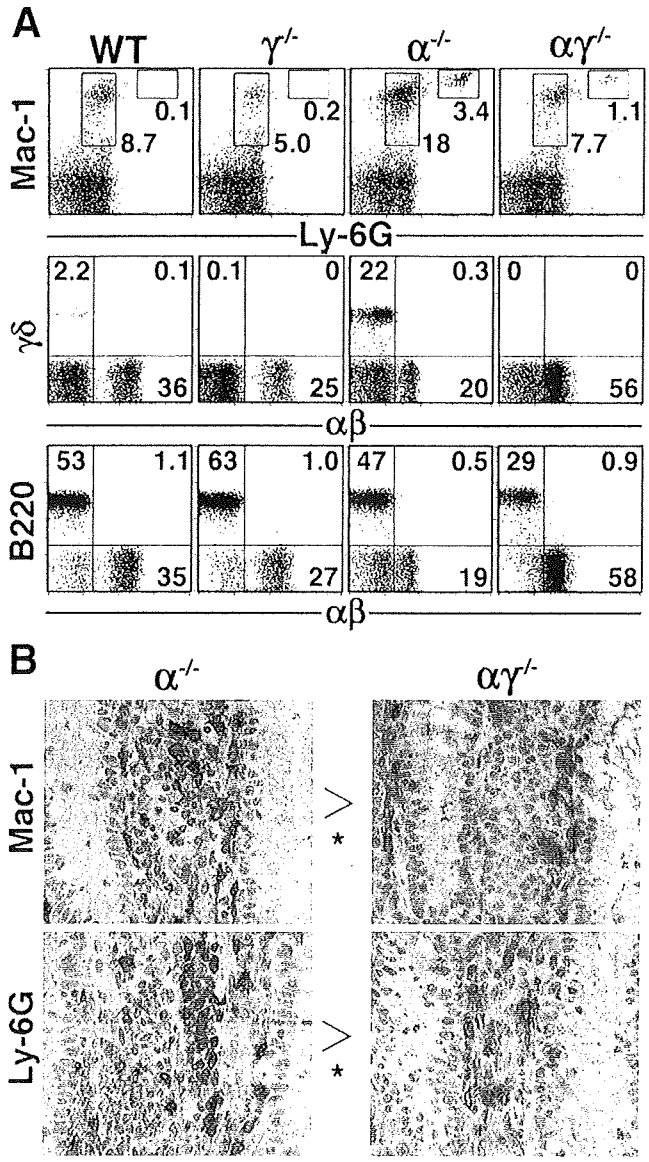

Figure 4. Decrease in colonic Mac-1$^+$Ly-6G$^-$ and Mac-1$^+$Ly-6G$^+$ cells in the absence of γδ T cells. WT (n = 3), $\gamma^{-/-}$ (n = 3), $\alpha^{-/-}$ (n = 4), and $\alpha\gamma^{-/-}$ (n = 4) mice from 28 weeks of age were examined. (*A*) Flow cytometric profiles of colonic LP cells. Absolute numbers of LP cells isolated from these WT, $\gamma^{-/-}$, $\alpha^{-/-}$, and $\alpha\gamma^{-/-}$ individuals were 5.1 × 10^5, 6.1 × 10^5, 32.3 × 10^5 and 12.0 × 10^5, respectively. (*B*) Representative immunohistochemical verification of the prominent infiltrations of Mac-1$^+$ and Ly-6G$^+$ cells into the inflamed colonic LP of $\alpha^{-/-}$ mice. Five tissue sections prepared from ascending colon to rectum per mouse, namely, 20 sections obtained from inflamed large intestines of $\alpha^{-/-}$ mice and those obtained from inflamed large intestines of $\alpha\gamma^{-/-}$ mice, were examined in a blinded fashion by 5 independent investigators, and the statistical difference in absolute numbers of Mac-1$^+$ and Ly-6G$^+$ cells between large intestinal mucosa from $\alpha^{-/-}$ and $\alpha\gamma^{-/-}$ mice were determined by 2-sided Mann–Whitney *U* test. *$P < .05$.

RT-PCR analysis and measurement of the amounts of representative proinflammatory cytokines as well as chemokines were performed to dissect further the role of γδ T cells in the UC-like colitis in $\alpha^{-/-}$ mice.

To this end, messenger RNA (mRNA) and proteins prepared from the large intestines of WT, $\gamma^{-/-}$, $\alpha^{-/-}$, and $\alpha\gamma^{-/-}$ mice were examined. Inflamed colonic tissues from $\alpha^{-/-}$ and $\alpha\gamma^{-/-}$ mice contained at least 10 times higher levels of cytokine (Table 1)- and chemokine (Table 2)-specific mRNA than those of WT and $\gamma^{-/-}$ mice except for IL-7 and IL-10 mRNA. In contrast to the mRNA from colonic tissues of $\alpha^{-/-}$ mice, those of $\alpha\gamma^{-/-}$ mice contained significantly smaller amounts of cytokine (TNF-α, IL-1β, IL-6, and TGF-β)- and chemokine (KC and MIP-2)-specific mRNA. With these observations in mind, we measured the amounts of representative cytokines as well as chemokines that had exhibited the differences in mRNA levels between the colonic tissues of $\alpha^{-/-}$ and $\alpha\gamma^{-/-}$ mice. First, in situ production of TNF-α, IL-1β, and IL-6 but not TGF-β proteins was significantly downregulated in the inflamed colonic mucosa of $\alpha\gamma^{-/-}$ mice as compared with that of $\alpha^{-/-}$ mice (Table 1). Second, KC and MIP-2 chemokines that are involved in the chemoattract of neutrophils and/or monocytes[23] were significantly decreased in large intestines of $\alpha\gamma^{-/-}$ mice compared with those in large intestines of $\alpha^{-/-}$ mice (Table 2).

To investigate the cell types responsible for the increases in these proinflammatory cytokines and chemokines, real-time RT-PCR analysis of mRNA present in the purified cell subsets from the inflamed colonic LP of $\alpha^{-/-}$ and $\alpha\gamma^{-/-}$ mice was performed (see Supplementary Figure 1 online at www.gastrojournal.org). The IL-1β and MIP-2 mRNA were expressed preferentially by Gr-1$^+$ cells, F4/80$^+$ cells, and CD11c$^+$ cells in the colon, whereas IL-6 mRNA was mainly expressed by Gr-1$^-$F4/80$^-$CD11c$^-$ cell populations. Expression levels of TNF-α- and KC-specific mRNA were comparable between all cell populations (Gr-1$^+$ cells, F4/80$^+$ cells, CD11c$^+$ cells, and Gr-1$^-$F4/80$^-$CD11c$^-$ cells) examined. Finally, the expression levels of these cytokine- and chemokine-specific mRNA in every cell subset were lower in cells from $\alpha\gamma^{-/-}$ mice than those in cells from $\alpha^{-/-}$ mice (see Supplementary Figure 1 online at www.gastrojournal.org).

Discussion

The $\alpha^{-/-}$ mice spontaneously develop colitis that shares many features with human UC.[16,24] Commensal enteric flora is required for the development of this colitis as indicated by the absence of colitis in $\alpha^{-/-}$ mice that are maintained under germ-free conditions.[22,25] The number of colonic γδ T cells drastically decreases in the $\alpha^{-/-}$ mice under germ-free conditions.[22] However, the study to identify the role of γδ T cells in the UC-like chronic colitis in $\alpha^{-/-}$ mice has been hampered by the difficulty in generating TCRαδ double mutant ($\alpha\delta^{-/-}$) mice because of the genomic organization of these TCR genes.[20] In the present study, we overcame this problem by newly generating $\gamma^{-/-}$ mice and subsequently crossing these mice with $\alpha^{-/-}$ mice to generate TCRα double mutant mice that lacked γδ T cells. By using these $\alpha\gamma^{-/-}$ mice, we herein provide a novel insight into the role of γδ T cells

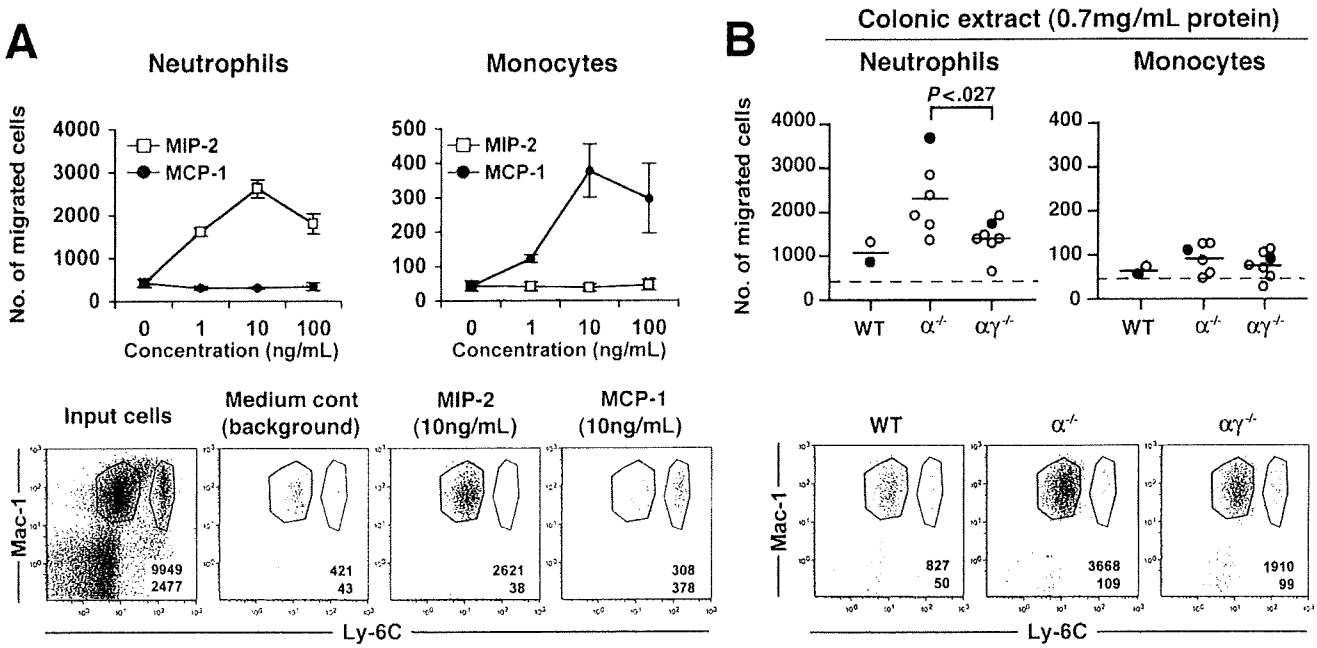

Figure 5. Chemotactic activity of colonic extracts from WT, $\alpha^{-/-}$, and $\alpha\gamma^{-/-}$ mice to neutrophils and monocytes. (*A*) The number of neutrophils and monocytes migrated in response to the increasing concentration of MIP-2 (*open square*) and MCP-1 (*solid circle*). The representative flow cytometric profiles are shown in the *lower panels*, and *red* and *blue gates* indicate the neutrophils and monocytes, respectively. *Colored numbers* represent means of the number of cells in each gate. (*B*) Chemotactic responses of neutophils and monocytes to colonic extracts (0.7 mg/mL protein) from WT, $\alpha^{-/-}$, and $\alpha\gamma^{-/-}$ mice, and each *circle* represents an individual mouse. *Horizontal bars* show mean values, and *dotted lines* indicate the number of migrated cells in medium alone. The representative flow cytomeric profiles of 3 individual animals indicated by the *solid red* and *blue circles* (*upper panels*) are shown in the *lower panels*, and *red* and *blue gates* indicate the neutrophils and monocytes, respectively.

that contributes to the exacerbation of UC-like colitis in $\alpha^{-/-}$ mice.

There is growing evidence supporting the fact that γδ T cells are part of the innate immune system and play an active multifaceted immunoregulatory role in the coordinated innate and acquired immune responses that maintain the integrity of many organs containing epithelia.[1,5,26,27] Nevertheless, the details of γδ T-cell functions are still not well understood as compared with those of αβ T cells. γδ T cells might play a defensive role against infections by various pathogenic microorganisms because exaggerated and severe infectious diseases occur in $\delta^{-/-}$ mice.[28-33] However, the same $\delta^{-/-}$ mice have also been demonstrated to display an increased host resistance to infection.[34,35] With regard to this, it is noteworthy that $V\gamma1^{+}$ γδ T cells are reported to eliminate the

Table 1. Real-Time RT-PCR Analysis and ELISA Assay of Cytokines in the Colonic Tissues

	Cytokine							
Mice (n)	TNF-α	IL-1β	IL-6	TGF-β	IFN-γ	IL-7	IL-10	IL-12
RT-PCR (copies per 10^3 HPRT)								
WT (5)	11.4 ± 0.53	6.86 ± 0.55	2.45 ± 0.64	123 ± 14.6	ND	11.7 ± 1.03	2.63 ± 0.28	0.82 ± 0.21
$\gamma^{-/-}$ (5)	9.20 ± 0.76	6.01 ± 0.61	2.14 ± 0.88	106 ± 10.7	ND	10.2 ± 0.78	2.09 ± 0.31	0.33 ± 0.09
$\alpha^{-/-}$ (7)	457 ± 35.7**	260 ± 18.6***	7.06 ± 1.04*	538 ± 48.6*	64.4 ± 8.90	11.0 ± 0.89	4.99 ± 0.72	9.58 ± 1.67
$\alpha\gamma^{-/-}$ (6)	205 ± 51.8**	98.5 ± 21.4***	2.93 ± 0.73*	319 ± 57.4*	45.0 ± 15.6	9.29 ± 1.11	6.42 ± 2.11	6.63 ± 1.01
ELISA (pg/mg protein)								
$\alpha^{-/-}$ (7)	100 ± 12.2**	975 ± 70.1**	8.24 ± 1.39**	2.09 ± 0.11	8.34 ± 1.50			
$\alpha\gamma^{-/-}$ (6)	27.0 ± 8.28**	647 ± 24.6**	2.92 ± 0.52**	2.57 ± 0.31	5.92 ± 2.56			

NOTE. All results are expressed as mean ± SE.
*$P < .05$.
**$P < .01$.
***$P < .001$.
ND, not detected

Table 2. Real-Time RT-PCR Analysis and ELISA Assay of Chemokines in the Colonic Tissues

	Chemokine					
Mice (n)	KC	MIP-2	GCP-2	MCP-1	MIP-1α	MIP-1β
RT-PCR (copies per 10^3 HPRT)						
WT (5)	6.05 ± 1.38	0.23 ± 0.01	12.3 ± 4.11	1.67 ± 0.17	0.78 ± 0.07	1.36 ± 0.22
$\gamma^{-/-}$ (5)	11.8 ± 1.19	0.22 ± 0.03	4.03 ± 1.49	1.77 ± 0.26	0.80 ± 0.04	1.42 ± 0.11
$\alpha^{-/-}$ (7)	382 ± 88.6*	101 ± 12.8**	721 ± 136	23.3 ± 4.37	35.0 ± 3.01	19.8 ± 0.88
$\alpha\gamma^{-/-}$ (6)	65.2 ± 17.4*	28.0 ± 9.80**	307 ± 168	16.0 ± 4.11	23.9 ± 7.34	14.2 ± 3.97
ELISA (pg/mg protein)						
$\alpha^{-/-}$ (7)	144 ± 22.4**	113 ± 21.2*	737 ± 139			
$\alpha\gamma^{-/-}$ (6)	32.4 ± 13.4**	44.9 ± 14.0*	414 ± 219			

NOTE. All results are expressed as mean ± SE.
*$P < .05$.
**$P < .01$.

macrophages infected with *Listeria monocytogenes*, whereas γδ T cells using Vγ elements other than Vγ1 gene appear to lack the ability to control macrophages but possess the ability to protect hosts from the infection-induced tissue injury.[36,37] In contrast to the beneficial function of γδ T cells by virtue of the fact that they can maintain the homeostasis of different types of organs,[1-5,8,27] a deleterious effect of γδ T cells on the regulation of neutrophil-mediated tissue damage after thermal (postburn) injury has been reported.[38] In various chronic and/or autoimmune inflammatory diseases, such as collagen-induced arthritis in mice[39] and murine insulin-dependent diabetes,[40] γδ T cells have been shown to exert a protective effect. Conversely, γδ T cells may directly contribute to autoimmune pathology of murine experimental allergic encephalomyelitis[41] as well as lupus in MRL/lpr mice.[42] Overall, both the beneficial and detrimental roles of γδ T cells in inflammatory process are evident.[43]

In chemically induced acute intestinal inflammation models (2,4,6-trinitrobenzene sulfonic acid- or dextran sulfate sodium-induced colitis), γδ T cells have been reported to play a protective role.[11-14] Depletion of γδ T cells by administration of anti-TCRγδ mAb into $TNF^{\Delta ARE}$ mice with a high frequency of spontaneous ileitis[44] did not lead to any histologic changes of ileitis.[45] However, transfer of bone marrow-derived γδ T cells has been shown to induce CD-like colitis in the bone marrow transplanted CD3εtg colitis model.[46] Although the role of γδ T cells in spontaneous chronic colitis remains to be explored to date, the results of the present study demonstrate the exacerbating effect of γδ T cells on the UC-like chronic colitis in $\alpha^{-/-}$ mice (Figures 3 and 4 and Tables 1 and 2). Interestingly, approximately 20% of $\alpha^{-/-}$ mice during 20 to 60 weeks of age suffered from ARP, whereas none of age-matched $\alpha\gamma^{-/-}$ mice showed ARP (Figure 3*D*). Of note, there were no differences in the age of onset of colitis and in the incidence of colitis (~80%) among 20- to 32-week-old $\alpha^{-/-}$ and $\alpha\gamma^{-/-}$ mice, but much more severe colitis was observed in $\alpha^{-/-}$ mice as compared with $\alpha\gamma^{-/-}$ mice. Therefore, it is possible that ARP may reflect increased severity of colitis and that γδ T cells may participate in the development of ARP.

Absence of γδ T cells in $\alpha\gamma^{-/-}$ mice leads to a significantly reduced production of TNF-α, IL-1β, and IL-6 proteins in the colonic tissues. These findings are consistent with our previous results[24] showing the involvement of TNF-α, IL-1β, and IL-6 in the perpetuation of inflammatory process in $\alpha^{-/-}$ mice. These inflammatory mediators have been shown to be important for host defense and wound repair.[47] Both KC and MIP-2 attract neutrophils to inflamed sites, and, in certain microbial infection, the collection of neutrophils leads to suppuration reflecting an active and vigorous host response against microbes. We also confirmed that colonic extracts from $\alpha\gamma^{-/-}$ mice exhibited the significantly weaker chemotactic activity to neutrophils than those from $\alpha^{-/-}$ mice. KC and MIP-2 mRNA expressions were lower in all purified cell subsets ($Gr\text{-}1^+$, $F4/80^+$, $CD11c^+$, and $Gr\text{-}1^-F4/80^-CD11c^-$ cells) from $\alpha\gamma^{-/-}$ mice than those from $\alpha^{-/-}$ mice. Therefore, in the presence of γδ T cells, many types of immune cells may be triggered to produce more chemokines, followed by infiltration of neutrophils into the colonic mucosa in $\alpha^{-/-}$ mice. γδ T-cell responsiveness that is manifested by recruitment and activation of inflammatory cells in which neutrophils predominate has also been reported.[1,31] In this context, it is of importance to note that the activity and severity of UC patients with increase in γδ T cells in the inflamed mucosa[9,10] (Figure 1) can be judged by the activation state of neutrophils in circulation[48] as well as by regional accumulation of neutrophils in the colonic crypt walls (cryptitis) or in the lumen of crypts (crypt abscess).[49]

The suppressive role of B cells[50] and the aggravating role of $TCR\beta^{dim}$ T cells[22,51] in the pathogenesis of colitis in $\alpha^{-/-}$ mice have been reported. Therefore, it is possible that γδ T cells may contribute to the exacerbation of this colitis by dampening regulatory B-cell function or by cooperating the colitogenic $TCR\beta^{dim}$ T cells. The possible complicated mechanism remains to be explored in the future. Levels of TNF-α and IL-1β mRNA in $F4/80^+$ cells

are higher in $\alpha^{-/-}$ mice compared with $\alpha\gamma^{-/-}$ mice (see Supplementary Figure 1 online at www.gastrojournal.org), suggesting that γδ T cells may activate macrophages to secrete large amounts of proinflammatory cytokines.

In conclusion, although γδ T cells at the inflamed colonic LP of $\alpha^{-/-}$ mice may protect intestinal epithelial injury, proinflammatory cytokines and neutrophil- and/or monocyte-chemoattractant chemokines induced by γδ T cells may directly and/or indirectly contribute to increased severity of UC-like chronic colitis in $\alpha^{-/-}$ mice. Further understanding of the molecular mechanisms of γδ T cell-mediated exacerbation of colitis in $\alpha^{-/-}$ mice will lead us to work out better therapeutic strategies for human UC.

Supplementary Data

Note: To access the supplementary material accompanying this article, visit the online version of *Gastroenterology* at www.gastrojournal.org, and at doi: 10.1053/j.gastro.2007.11.056.

References

1. Hayday A, Tigelaar R. Immunoregulation in the tissues by γδ T cells. Nat Rev Immunol 2003;13:233–242.
2. Jameson J, Ugarte K, Chen N, et al. A role for skin γδ T cells in wound repair. Science 2002;296:747–749.
3. Boismenu R, Havran WL. Modulation of epithelial cell growth by intraepithelial γδ T cells. Science 1994;266:1253–1255.
4. Komano H, Fijiura Y, Kawaguchi M, et al. Homeostatic regulation of intestinal epithelia by intraepithelial γδ T cells. Proc Natl Acad Sci USA 1995;92:6147–6151.
5. Mak TW, Ferrick DA. The γδ T-cell bridge: linking innate and acquired immunity. Nat Med 1998;4:764–765.
6. Podolsky DK. Inflammatory bowel disease. N Engl J Med 2002; 347:417–429.
7. Targan SR, Karp LC. Defects in mucosal immunity leading to ulcerative colitis. Immunol Rev 2005;206:296–305.
8. Shiohara T, Moriya N, Hayakawa J, et al. Resistance to cutaneous graft vs host disease is not induced in T-cell receptor δ gene-mutant mice. J Exp Med 1996;183:1483–1489.
9. McVay LD, Li B, Biancaniello R, et al. Changes in human mucosal γδ T cell repertoire and function associated with the disease process in inflammatory bowel disease. Mol Med 1997;3:183–203.
10. Yeung MM-W, Melgar S, Baranov V, et al. Characterization of mucosal lymphoid aggregates in ulcerative colitis: immune cell phenotype and TCR-γδ expression. Gut 2000;47:215–227.
11. Hoffmann JC, Peters K, Henschke S, et al. Role of T lymphocytes in rat 2,4,6-trinitrobenzene sulphonic acid (TNBS) induced colitis: increased mortality after γδ T cell depletion and no effect of αβ T cell depletion. Gut 2001;48:489–495.
12. Inagaki-Ohara K, Chinen T, Matsuzaki G, et al. Mucosal T cells bearing TCRγδ play a protective role in intestinal inflammation. J Immunol 2004;173:1390–1398.
13. Chen Y, Chou K, Fuchs E, et al. Protection of the intestinal mucosa by intraepithelial γδ T cells. Proc Natl Acad Sci U S A 2002;99:14338–14343.
14. Tsuchiya T, Fukuda S, Hamada H, et al. Role of γδ T cells in the inflammatory response of experimental colitis mice. J Immunol 2003;171:5507–5513.
15. Mizoguchi A, Mizoguchi E, Chiba C, et al. Cytokine imbalance and autoantibody production in T cell receptor-α mutant mice with inflammatory bowel disease. J Exp Med 1996;183:847–856.
16. Mombaerts P, Mizoguchi E, Grusby MJ, et al. Spontaneous development of inflammatory bowel disease in T cell receptor mutant mice. Cell 1993;75:274–282.
17. Hokama A, Mizoguchi E, Sugimoto K, et al. Induced reactivity of intestinal $CD4^+$ T cells with an epithelial cell lectin, galectin-4, contributes to exacerbation of intestinal inflammation. Immunity 2004;20:681–693.
18. de Bruijn MF, van Vianen W, Ploemacher RE, et al. Bone marrow cellular composition in *Listeria monocytogenes* infected mice detected using ER-MP12 and ER-MP20 antibodies: a flow cytometric alternative to different counting. J Immunol Methods 1998;217:27–39.
19. Itohara S, Mombaerts P, Lafaille J, et al. T cell receptor δ gene mutant mice: independent generation of αβ T cells and programmed rearrangements of γδ TCR genes. Cell 1993;72:337–348.
20. Davis MM, Bjorkman PJ. T-cell antigen receptor genes and T-cell recognition. Nature 1988;334:395–402.
21. Goren I, Kampfer H, Muller E, et al. Oncostatin M expression is functionally connected to neutrophils in the early inflammation phase of skin repair: implications for normal and diabetes-impaired wounds. J Invest Dermatol 2006;126:628–637.
22. Kawaguchi-Miyashita M, Shimada S, Kurosu H, et al. An accessory role of $TCR\gamma\delta^+$ cells in the exacerbation of inflammatory bowel disease in TCRα mutant mice. Eur J Immunol 2001;31: 980–988.
23. Charo IF, Ransohoff RM. The many roles of chemokines and chemokine receptors in inflammation. N Engl J Med 2006;354: 610–621.
24. Mizoguchi A, Mizoguchi E, Bhan AK. Immune networks in animal models of inflammatory bowel disease. Inflamm Bowel Dis 2003; 9:246–259.
25. Dianda L, Hanby AM, Wright NA, et al. T cell receptor-αβ-deficient mice fail to develop colitis in the absence of a microbial environment. Am J Pathol 1997;150:91–97.
26. Tonegawa S, Berns A, Bonneville M, et al. Diversity, development, and probable functions of γδ T cells. Cold Spring Harbor Symp Quant Biol 1989;54:31–44.
27. Havran WL. A role for epithelial γδ T cells in tissue repair. Immunol Res 2000;21:63–69.
28. Mombaerts P, Arnoldi J, Russ F, et al. Different roles of αβ and γδ T cells in immunity against an intracellular bacterial pathogen. Nature 1993;365:53–56.
29. Roberts SJ, Smith AL, Wet AB, et al. T-cell $\alpha\beta^+$ and $\gamma\delta^+$ deficient mice display abnormal but distinct phenotypes toward a natural, widespread infection of the intestinal epithelium. Proc Natl Acad Sci U S A 1996;93:11774–11779.
30. D'Souza CD, Cooper AM, Frank AA, et al. An anti-inflammatory role for γδ T lymphocytes in acquired immunity to *Mycobacterium tuberculosis*. J Immunol 1997;158:1217–1221.
31. King DP, Hyde DM, Jackson KA, et al. Cutting edge: protective response to pulmonary injury requires γδ lymphocytes. J Immunol 1999;162:5033–5036.
32. Moore TA, Moore BB, Newstead NW, et al. γδ-T cells are critical for survival and early proinflammatory cytokine gene expression during murine *Klebsiella* pneumonia. J Immunol 2000;165: 2643–2650.
33. Selin LK, Santolucito PA, Pinto AK, et al. Innate immunity to viruses: control of vaccinia virus infection by γδ T cells. J Immunol 2001;166:6784–6794.
34. Emoto M, Nishimura H, Sakai T, et al. Mice deficient in γδ T cells are resistant to lethal infection with *Salmonella choleraesuis*. Infect Immun 1995;63:3736–3738.

35. Uezu K, Kawakami K, Miyagi K, et al. Accumulation of γδ T cells in the lungs and their regulatory roles in Th1 response and host defense against pulmonary infection with *Cryptococcus neoformans*. J Immunol 2004;172:7629–7634.
36. Andrew EM, Newton DJ, Dalton JE, et al. Delineation of the function of a major γδ T cell subset during infection. J Immunol 2005;175:1741–1750.
37. Newton DJ, Andrew EM, Dalton JE, et al. Identification of novel γδ T-cell subsets following bacterial infection in the absence of $V\gamma1^+$ T cells: homeostatic control of γδ T-cell responses to pathogen infection by $V\gamma1^+$ T cells. Infect Immun 2006;74: 1097–1105.
38. Toth B, Alexander M, Daniel T, et al. The role of γδ T cells in the regulation of neutrophil-mediated tissue damage after thermal injury. J Leukoc Biol 2004;76:545–552.
39. Peterman GM, Spencer C, Sperling AI, et al. Role of γδ T cells in murine collagen-induced arthritis. J Immunol 1993;151:6546–6558.
40. Harrison LC, Dempsey-Collier M, Kramer DR, et al. Aerosol insulin induces regulatory CD8 γδ T cells that prevent murine insulin-dependent diabetes. J Exp Med 1996;184:2167–2174.
41. Rajan AJ, Gao Y-L, Raine CS, et al. A pathogenic role of γδ T cells in relapsing-remitting experimental allergic encephalomyelitis in the SJL mouse. J Immunol 1996;157:941–949.
42. Peng SL, Madaio MP, Highes DP, et al. Murine lupus in the absence of αβ T cells. J Immunol 1996;156:4041–4049.
43. Hayday A, Geng L. γδ cells regulate autoimmunity. Curr Opin Immunol 1997;9:884–889.
44. Kontoyiannis D, Pasparakis M, Piazzoro TT, et al. Impaired on/off regulation of TNF biosynthesis in mice lacking TNF AU-rich elements: implications for joint and gut-associated immunopathologies. Immunity 1999;10:387–398.
45. Kuhl AA, Loddenkemper C, Westermann J, et al. Role of γδ T cells in inflammatory bowel disease. Pathobiology 2002;70: 150–155.
46. Simpson SJ, Hollander GA, Mizoguchi E, et al. Expression of pro-inflammatory cytokines by $TCR\alpha\beta^+$ and $TCR\gamma\delta^+$ T cells in an experimental model of colitis. Eur J Immunol 1997;27: 17–25.
47. Nathan C. Points of control in inflammation. Nature 2002;420: 846–852.
48. Suematsu M, Suzuki M, Kitahora T, et al. Increased respiratory burst of leukocytes in inflammatory bowel diseases: the analysis of free radical generation by using chemiluminescence probe. J Clin Lab Immunol 1987;24:125–128.
49. Simmonds NJ, Allen RE, Stevens TR, et al. Chemiluminescence assay of mucosal reactive oxygen metabolites in inflammatory bowel disease. Gastroenterology 1992;103:186–196.
50. Sugimoto K, Ogawa A, Shimomura Y, et al. Inducible IL-12-producing B cells regulate Th2-mediated intestinal inflammation. Gastroenterology 2007;133:124–136.
51. Takahashi I, Kiyono H, Hamada S. $CD4^+$ T-cell population mediates development of inflammatory bowel disease in T-cell receptor α chain-deficient mice. Gastroenterology 1997;112:1876–1886.

Received April 11, 2007. Accepted November 15, 2007.

Address requests for reprints to: Hiromichi Ishikawa, MD, PhD, Department of Microbiology and Immunology, Keio University School of Medicine, 35 Shinanomachi, Shinjuku-ku, Tokyo 160-8582, Japan. e-mail: h-ishika@sc.itc.keio.ac.jp; fax: (81) 3-5360-1508.

Supported in part by a Grant-in-Aid for Creative Scientific Research, the Japan Society for the Promotion of Science (13GS0015); by Special Coordination Funds for Promoting Science and Technology from the Japanese Ministry of Education, Culture, Sports, Science, and Technology; and by Research on Specific Diseases, Japanese Ministry of Health, Labor, and Welfare (to H.I.); by Keio University Special Grant-in-Aid for Innovative Collaborative Research Projects (to T.H.); by National Institutes of Health grants DK47677 (to A.K.B.) and DK064351 (to A.M.); by the Center for the Study of Inflammatory Bowel Disease, Massachusetts General Hospital; and by 21st Century Center-of-Excellence (COE) Program for Life Science from MEXT (to M.S.).

The authors thank Dr Daniel K. Podolsky for his many valuable discussions and comments, Dr Leo Lefrancois for his critical reading of the manuscript, and Dr Atsuhiro Ogawa for his excellent technical assistance.

M.N. and Y.K. contributed equally to this work.

Y.K.'s current location is Department of Immunology, Kinki University School of Medicine, Osaka, Japan.

H.Y.'s current location is Health Research Foundation, Kyoto, Japan.

Conflicts of interest: No conflicts of interest exist.

T.N. was a research fellow supported by 21st Century COE Program for Life Science from MEXT and is now supported by Global COE Program for Human Metabolomic Systems Biology from MEXT (to M.S.).

GASTROENTEROLOGY 2008;135:142–151

BASIC—ALIMENTARY TRACT

DNA Hypermethylation Contributes to Incomplete Synthesis of Carbohydrate Determinants in Gastrointestinal Cancer

YUKI I. KAWAMURA,*,‡ MINORU TOYOTA,§, REI KAWASHIMA,* TERUKI HAGIWARA,* HIROMU SUZUKI,§ KOHZOH IMAI,§ YASUHISA SHINOMURA,§ TAKASHI TOKINO, REIJI KANNAGI,‡,¶ and TAEKO DOHI*,‡

*Department of Gastroenterology, Research Institute, International Medical Center of Japan, Tokyo, Japan; ‡CREST, Japan Science and Technology Agency, Kawaguchi, Japan; §First Department of Internal Medicine and Department of Molecular Biology, Cancer Research Institute, Sapporo Medical University, Sapporo, Japan; and the ¶Program of Molecular Pathology, Aichi Cancer Center, Nagoya, Japan

See editorial on page 305.

Background & Aims: **It has long been known that malignant transformation is associated with abnormal expression of carbohydrate determinants. The aim of this study was to clarify the cause of cancer-associated abnormal glycosylation in gastrointestinal (GI) cancers.** ***Methods:*** **We compared the expression levels of "glyco-genes," including glycosyltransferases and glycosidases, in normal GI mucosa and in gastric and colorectal cancer cells. To examine the possibility that DNA hypermethylation contributed to the down-regulation of these genes, we treated GI cancer cells with 5-aza-2′-deoxycytidine (5-aza-dC), an inhibitor of DNA methyltransferase.** ***Results:*** **The silencing of some of these glyco-genes, but not up-regulation of certain molecules, was observed. The Sd^a carbohydrate was abundantly expressed in the normal GI mucosa, but its expression was significantly decreased in cancer tissues. When human colon and gastric cancer cells were treated with 5-aza-dC, cell surface expression of Sd^a and the transcription of *B4GALNT2*, which catalyzes the synthesis of the Sd^a, were induced. The promoter region of the human *B4GALNT2* gene was heavily hypermethylated in many of the GI cancer cell lines examined as well as in gastric cancer tissues (39 out of 78 cases). In addition, aberrant methylation of the *B4GALNT2* gene was strongly correlated with Epstein-Barr virus-associated gastric carcinomas and occurred coincidentally with hypermethylation of the *ST3GAL6* gene.** ***Conclusions:*** **Epigenetic changes in a group of glycosyltransferases including *B4GALNT2* and *ST3GAL6* represent a malignant phenotype of gastric cancer caused by silencing of the activity of these enzymes, which action may eventually induce aberrant glycosylation and expression of cancer-associated carbohydrate antigens.**

It has long been known that malignant transformation is associated with abnormal expression of carbohydrate determinants.[1] Many glycosyl epitopes such as sialyl Tn, Tn, T, and sialyl Lewis x/a ($sLe^{x/a}$) have been reported to be cancer-associated antigens. Some of them show statistically significant correlations between the degree of their expression in cancer tissues and the postoperative prognosis of patients with many types of human cancers.[2–4] In addition, $sLe^{x/a}$ determinants are known to serve as ligands for E-selectin, which is inducibly expressed by endothelial cells, in hematogenous metastasis of cancers.[5,6] A long-standing debate is which is more important in understanding cancer-associated carbohydrate antigens, "neo-synthesis" or "incomplete synthesis." To verify the former hypothesis, the levels of many glycosyltransferases involved in "neo-synthesis" of tumor-related glycosyl epitopes and their mRNA expression have been studied; however, no conclusive results have been obtained to date.[7–9]

On the other hand, there is a group of carbohydrate determinants that is less expressed in cancer tissues when compared with their level in normal tissues. Because their structures are commonly more complicated, the concept of "incomplete synthesis," that the synthesis of complex carbohydrate determinants in nonmalignant cells might be impaired upon malignant transformation, has been proposed as an important cause of cancer-associated abnormal glycosylation.[10] The blood group Sd^a carbohydrate antigen serves as a typical example among the latter

Abbreviations used in this paper: 5-aza-dC, 5-aza-2′-deoxycytidine; COBRA, combined bisulfite restriction analysis; DNMT, DNA methyltransferase; EBV, Epstein-Barr virus; FUT, fucosyltransferase; Gal, galactose; GalNAc, *N*-acetylgalactosamine; GALNT, *N*-acetylgalactosaminyltransferase; GAPDH, glyceraldehyde-3-phosphate dehydrogenase; GI, gastrointestinal; mAb, monoclonal antibody; HP, *Helicobacter pylori*; Sd^a- 1, 4GalNAcT, 1,4*N*-acetylgalactosaminyltransferase, which forms Sd^a carbohydrate determinants; ST, sialyltransferase; type II precursor, Gal 1,4GlcNAc-R.

0016-5085/08/$34.00
doi:10.1053/j.gastro.2008.03.031

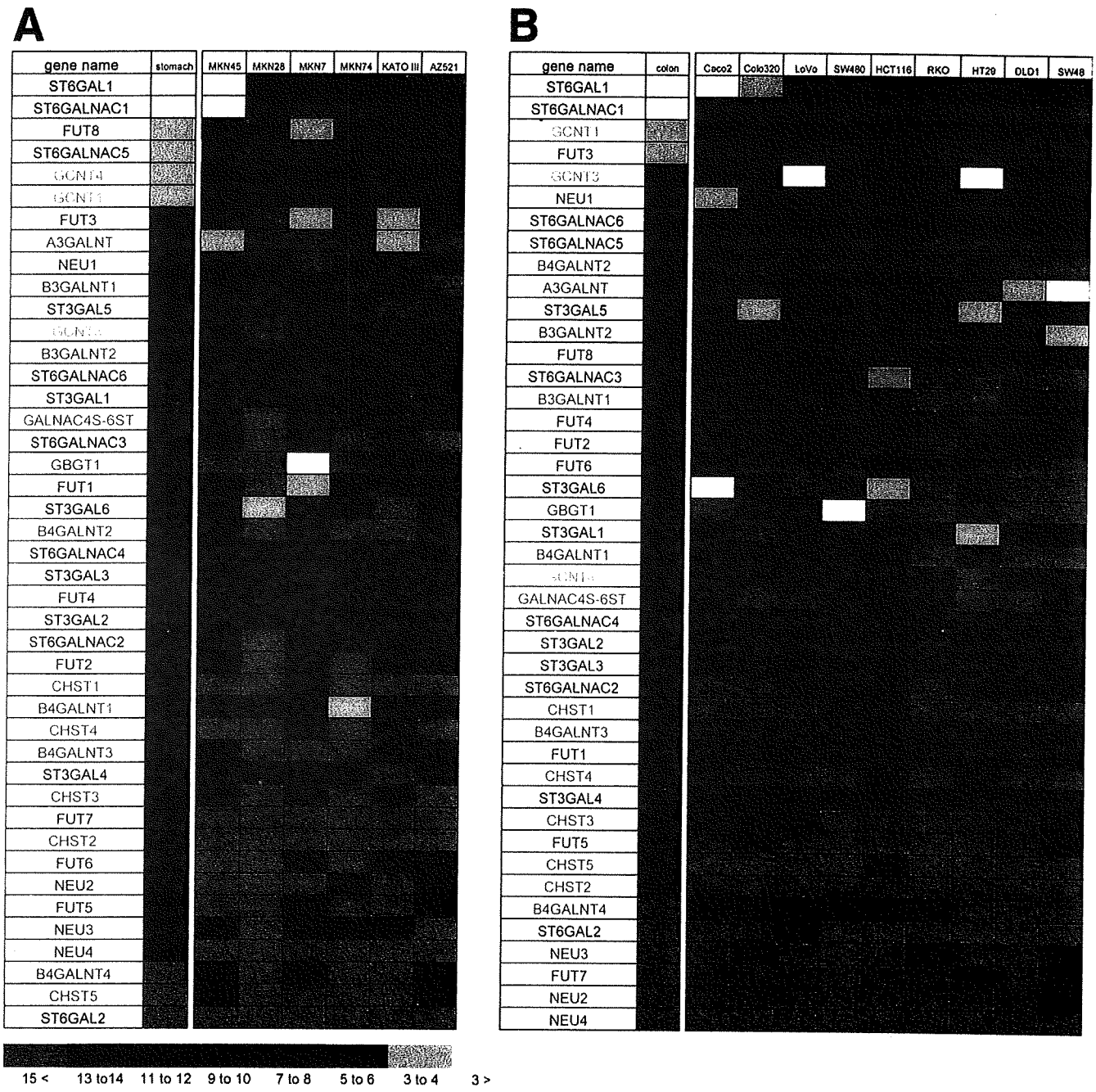

Figure 1. Profiles of expression of glycosylation-related genes in human GI tissues and cancer cell lines. Quantitative PCR analysis was carried out on normal human stomach and gastric cancer cell lines (*A*) and on normal human colon and CRC cell lines (*B*). Human glyco-genes, encoding 8 fucosyltransferases (classified by *blue*), 8 *N*-acetylgalactosaminyltransferase genes (*red*), 3 *N*-acetylglucosaminyltransferase genes (*orange*), 14 sialyltransferase genes (*black*), 6 sulfotransferase genes (*green*), and 4 sialidase genes (*purple*) were examined. Expression levels of each gene were sorted according to Ct (see Materials and Methods) calibrated by using GAPDH and visualized by color as indicated by the bar below.

group. This carbohydrate determinant is abundantly expressed on glycolipids and glycoproteins in the normal gastrointestinal (GI) tract mucosa in the majority of humans; however, its expression in cancer tissue is strikingly reduced or absent.[11,12] The last step in the biosynthesis of Sd^a is catalyzed by 1,4-*N*-acetylgalactosaminyl-transferase (1,4GalNAcT). The activity of the 1,4GalNAcT responsible for synthesizing the Sd^a determinant (Sd^a- 1,4GalNAcT) also dramatically decreases in gastric and colonic cancer tissue.[13,14] Recently we reported that forced expression of Sd^a- 1,4GalNAcT in GI cancer cells reduced their expression of $sLe^{x/a}$ carbohydrates and decreased their metastatic potential in nude mice, probably owing to competition with $sLe^{x/a}$ synthases for acceptor carbohydrate.[15] Thus, the lack of Sd^a antigens in cancer cells is functionally important;

however, very little is known about the molecular mechanism underlying the regulation of Sd^a expression.

In line with these hypotheses of "neo-synthesis" and "incomplete synthesis," we compared the expression of "glyco-genes," including glycosyltransferases and glycosidases, in normal GI mucosa with that in gastric and colorectal cancer (CRC) cells in this study. Recently, epigenetic changes, such as DNA hypermethylation, have been recognized as one of the important mechanisms for gene inactivation.[16] In this study, we investigated the possible role of aberrant methylation in the glycosyltransferase gene promoter region in human GI cancer cells. We also examined epigenetic changes in a group of glycosyltransferases in human gastric cancer tissues and analyzed their relation to clinicopathologic features of the cases.

Materials and Methods

Cell Lines and Specimens

The gastric and colon carcinoma cell lines that were used in this study were obtained from the Japanese Collection of Research Bioresources (Tokyo, Japan) or the American Tissue Type Collection (Manassas, VA). Human CRC cell line HCT116 with genetic disruption of DNMT1 (DNMT1 KO) or both DNMT1 and DNMT3b (DKO) were established as described previously.[17] The 78 gastric tumor specimens and their paired normal tissue specimens were obtained from 78 randomly selected Japanese patients. Informed consent was obtained from all patients before the samples were collected.

Reverse Transcription-Polymerase Chain Reaction

Quantitative polymerase chain reaction (PCR) of glyco-genes was performed by using ABI TaqMan probes (Applied Biosystems, Foster City, CA) as described previously.[18,19] Threshold cycle numbers (Ct) were determined with Sequence Detector software and transformed by using the Ct method as described by the manufacturer, with *glyceraldehyde-3-phosphate dehydrogenase* (GAPDH) used as the calibrator gene. Human glyco-genes examined in this study, 8 genes encoding fucosyltransferases (*FUT1, FUT2, FUT3, FUT4, FUT5, FUT6, FUT7,* and *FUT8*), 8 *N*-acetylgalactosaminyltransferase genes (*A3GALNT, GBGT1, B3GALNT1, B3GALNT2, B4GALNT1, B4GALNT2, B4GALNT3,* and *B4GALNT4*), 3 *N*-acetylglucosaminyltransferase genes (*GCNT1, GCNT3,* and *GCNT4*), 14 sialyltransferase genes (*ST3GAL1, ST3GAL2, ST3GAL3, ST3GAL4, ST3GAL5, ST3GAL6, ST6GAL1, ST6GAL2, ST6GALNAC1, ST6GALNAC2, ST6GALNAC3, ST6GALNAC4, ST6GALNAC5,* and *ST6GALNAC6*), 6 sulfotransferase genes (*GALNAC4S-6ST, CHST1, CHST2, CHST3, CHST4* and *GCNT5*), and 4 sialidase genes (*NEU1, NEU2, NEU3,* and *NEU4*), and TaqMan probe kits used in this study are summarized in Supplementary Table 1 (see supplementary material online at www.gastrojournal.org). Human stomach and colon total RNA (BioChain, Hayward, CA) were used as normal controls; they were prepared from normal stomachs and colon mucosae pooled from healthy subjects.

Flow Cytometry

Flow cytometry was performed with a FACScan (BD Bioscience, Franklin Lakes, NJ). Monoclonal antibody (mAb) KM694 (directed against Sd^a) was provided by Tokyo Research Laboratories (Kyowa Hakko Kogyo Co, Ltd. Tokyo, Japan).

Combined Bisulfite Restriction Analysis and Bisulfite Sequencing

We assessed gene methylation by using primers that were designed to amplify both the methylated and unmethylated alleles.[20] Bisulfite modification was carried out by using an EpiTect Bisulfite Kit (Qiagen, Tokyo, Japan). For combined bisulfite restriction analysis (COBRA), the PCR primers used for B4GALNT2 were 5′-ATTGGTTTTTYGTATAGGTGGTTG-3′ and 5′-CCRAACCRATTCCCACACTC-3′, yielding a PCR product of 174 bp. Primers for ST3GAL6[21] were 5′-GTTTGTTATATYGGGTYGTAGAAG-3′ and 5′-AATTAAAACTAACRAAAACCTAAAACT-3′ (162 bp). The products were then digested with the restriction endonuclease Hha*I* (for *B4GALNT2*) or AfaI (for *ST3GAL6*), which cleave only methylated CpG sites. For bisulfite sequencing, the PCR primers used for B4GALNT2 were 5′-GAGAGGTGAAATTTYGGGAGTA-3′ and 5′-RACTATCCACAACCCRCAATC-3′ (430 bp). For sequencing of the bisulfite-PCR product, the DNA fragment was purified and cloned into pCR4-TOPO vector (Invitrogen, Carlsbad, CA). Clones for subsequent sequencing were randomly picked up.

Detection of the Epstein–Barr Virus Genome and Helicobacter pylori

To detect the Epstein-Barr virus (EBV) genome in gastric tumors, we performed real-time PCR using 2 sets of primers as described previously.[22] Consistent results were obtained with both systems. *Helicobacter pylori* (HP) infection was identified by conducting histologic review of hematoxylin and eosin-stained tissue specimens and PCR assays as described by Clayton et al.[23]

Mutation Analysis

Genomic DNA was amplified by using exon-specific primers for p53 exons 2–11 and the mutations were examined as described previously.[24]

Immunohistochemical Analysis

Frozen sections of 8- m thickness were prepared from a surgical specimen. After blocking sections with 3% bovine serum albumin in phosphate-buffered saline and then incubating them with mAb KM694, bound mAbs were detected with fluorescein isothiocyanate-conjugated goat anti-mouse immunoglobulin M (Southern Biotechnology Associates, Inc, Birmingham, AL).

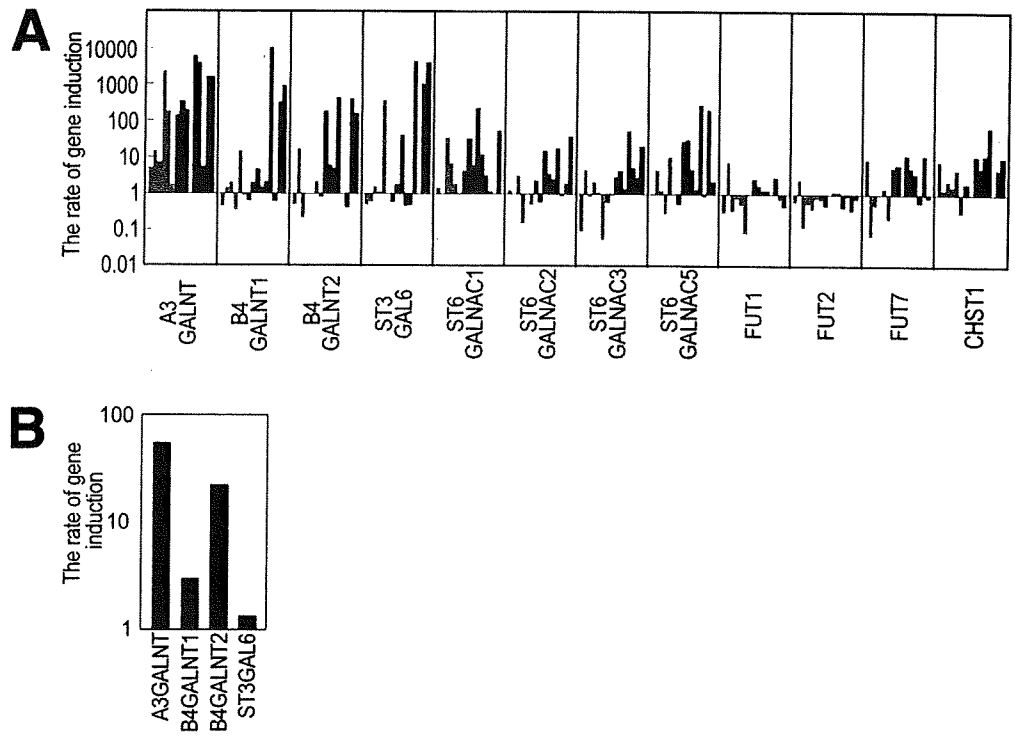

Figure 2. Expression of glycosylation-related genes in DNA methyltransferase-inhibited cells. (*A*) Six human gastric cancer (MKN45, MKN28, MKN7, MKN74, KATO III, and AZ521, as depicted in order from left to right by the *gray bars*) and 9 CRC (Caco2, Colo320, LoVo, SW480, HCT116, RKO, HT29, DLD1, and SW48, as depicted in order from left to right by the *black bars*) cell lines were treated with 2 mol/L 5-aza-dC for 72 hours, and the expression level of each gene was then assessed by RT-PCR. The rate of induction is expressed as the ratio of treated to untreated cells. The genes that were analyzed are shown at the bottom of the bar graph. (*B*) RNA was harvested from HCT116 and DKO cells, and the expression level of each of the indicated genes was assessed by RT-PCR. The rate of induction is expressed as the ratio of induction in DKO cells to that in the parental HCT116 cells.

Statistical Analysis

Each tumor was classified based on tumor location; macroscopic type; lymphatic invasion; venous invasion (Japanese Gastric Cancer Association)[25]; pathologic tumor, lymph node, metastasis (pTMN) classification[26]; and the Lauren classification.[27] Methylation of *B4GALNT2* was compared by using the Student *t*-test for age; the Mann-Whitney *U* test for tumor size, pT status, pN status, and disease stage; and the Fisher exact test for gender, tumor location, macroscopic type, histology, lymphatic invasion, venous invasion, pM status, EBV association, HP status, p53 mutation, and methylation of ST3GAL6. The Fisher exact test was carried out by using SAS (SAS Institute Inc, Cary, NC), and other statistical analyses were made with SPSS software (version 11.0; SPSS Inc, Chicago, IL). All tests were 2-tailed, and values of P .05 were considered significant.

Results

Expression of Genes Involved in the Synthesis and Modification of Carbohydrate Determinants in Human GI Tissue and Cancer Cells

It has been known that carbohydrate structures in GI cancers are quite different from those in normal GI epithelium. To clarify the cause of this abnormal glycosylation in GI cancer cells, we first examined the expression levels of 43 "glyco-genes," including 8 genes encoding fucosyltransferases, 14 sialyltransferase genes, 8 *N*-acetylgalactosaminyltransferase genes, 3 *N*-acetylglucosaminyltransferase genes, 6 sulfotransferase genes, and 4 sialidase genes (Supplementary Table 1). There was no gene whose expression was universally up-regulated in the GI cancer cell lines examined when compared with normal tissues. On the other hand, we found approximately one third of glycosyltransferase genes that were expressed in normal GI mucosa but whose expression levels were decreased in many GI cancer cell lines (Figure 1*A* and *B*). This silencing of glycosyltransferases was the major cancer-associated change detected in glyco-gene expression. To examine the possibility that DNA methylation contributed to the low expression levels of these genes, we chose 12 genes containing CpG islands in their promoter region from among cancer-associated down-regulated glyco-genes. When GI cancer cells were treated with 5-aza-2′-deoxycytidine (5-aza-dC), a DNA methyltransferase inhibitor, the mRNA expression of glycosyltransferases was significantly induced in many of them (Figure 2*A*). On the other hand, the expression of 2 glycosyltrans-

ferases (*FUT1* and *FUT2*) was not recovered by the 5-aza-dC-treatment, implying there might be certain glyco-genes whose expression was not controlled by DNA hypermethylation despite the presence of CpG islands. In the human CRC cell line HCT116 with genetic disruption of both *DNMT1* and *DNMT3b*,[17] in which genomic DNA methylation was nearly eliminated, the expression of *A3GALNT* and *B4GALNT2* was rescued (Figure 2*B*). Because it has been reported that promoter hypermethylation of the *A3GALNT* gene is associated with the loss of blood group A antigen expression in bladder cancer, oral squamous cell carcinoma, and gastric cancer cell lines,[28-30] our results suggest that aberrant methylation of the *A3GALNT* gene may lead to a cancer-associated reduction in the level of A antigen in colon cancers. Although remarkable induction of *B4GALNT1* mRNA was observed after 5-aza-dC-treatment, we excluded the *B4GALNT1* gene from subsequent analysis; because the expression of *B4GALNT1* and GM2 gangliosides synthesized by *B4GALNT1* is already known to be increased in GI cancers.[31] In any case, these results strongly suggest that down-regulation of glycosyltransferases might be the leading cause of cancer-associated abnormal glycosylation and that the *B4GALNT2* gene is a good representative of gene silencing by hypermethylation.

Recovery of Sd^a Carbohydrate Determinant in CRC Cells by Suppression of DNA Methyltransferases

The human *B4GALNT2* gene encodes a 1,4GalNAcT that is responsible for the synthesis of Sd^a carbohydrate antigen (Sd^a- 1,4GalNAcT). A noteworthy characteristic of the Sd^a carbohydrate determinant is that its expression is restricted to normal GI mucosa and is strikingly reduced or absent in GI cancer tissue.[11,12] So we asked if the membrane Sd^a structure could be detected in human CRC cell lines in which DNA methylation was suppressed. Treatment of T84 and HT29 human colonic cancer cell lines, which originally lacked the Sd^a carbohydrate, with 5-aza-dC resulted in an obvious increase in cell-surface expression of Sd^a along with the concomitant induction of *B4GALNT2* expression (Figure 3*A* and *B*). When these cells were treated with butyrate, a histone deacetylase inhibitor, neither expression of Sd^a antigen nor *B4GALNT2* mRNA was induced. We found that DNMT1 KO cells strongly expressed Sd^a determinants, whereas the parental HCT116 cells only weakly expressed it (Figure 3*C*). Furthermore, transcripts of *B4GALNT2* were detected in DNMT1 KO cells, but not in the parental HCT116 cells. These results suggest collectively that DNA hypermethylation rather than histone deacetylation may contribute to the down-regulation of *B4GALNT2* expression in cancer cells.

Methylation Status of B4GALNT2 *Gene Promoter Region in GI Cancer Cell Lines and Primary Gastric Carcinomas*

Next, we examined the methylation status of the upstream of the *B4GALNT2* gene in gastric cancer cell lines by COBRA. Hypermethylation in the *B4GALNT2* gene was detected in 5 of 6 human gastric cancer cell lines tested (Figure 4*A*, *left*). Atypical methylation in the *B4GALNT2* in a primary gastric carcinoma but not in the normal gastric mucosa adjacent to it was also found (Figure 4*A*, *right*). Because COBRA reflects the methylation status of only 2 adjoining CpG motifs, PCR products, extending from 169 bp upstream to 217 bp downstream from the translation start site and containing 39 CpGs, were subjected to bisulfite sequencing. Most of the CpGs examined were methylated in gastric cancer cells except in MKN45 cells, which were methylation negative by COBRA (Figure 4*B*). We also examined the methylation status of the *B4GALNT2* gene in DNMT1/

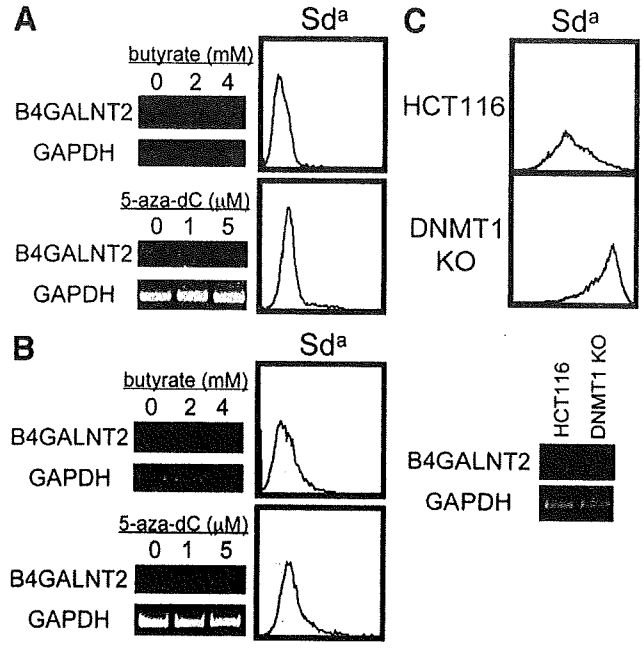

Figure 3. Effects of inhibitors on cell-surface Sd^a antigen and *B4GALNT2* mRNA expression in human CRC cells. Human CRC cell line T84 (*A*) and HT29 (*B*) were treated with the histone deacetylase inhibitor butyrate (*upper panels*) or the methyltransferase inhibitor 5-aza-dC at the concentrations indicated (*lower panels*). For RT-PCR analysis, cells were collected after 3 days of treatment, and expression levels of *B4GALNT2* and *GAPDH* were then assessed. For flow cytometric analysis, cells were treated with 4 mol/L butyrate (*upper panels*) or 5 mol/L 5-aza-dC (*lower panels*) for 6 days and then were stained with mAb KM694 (specific for Sd^a). Filled histograms represent the control staining of untreated cells. (*C*) Human CRC cell line HCT116 and DNMT1 KO cells were stained with mAb KM694 and then analyzed by flow cytometry. Filled histograms represent the control staining without mAb (*upper panels*). HCT116 and DNMT1 KO cells were also assessed for expression levels of *B4GALNT2* and *GAPDH* by RT-PCR (*lower panels*). The data are representative of 3 separate experiments, which gave similar results.

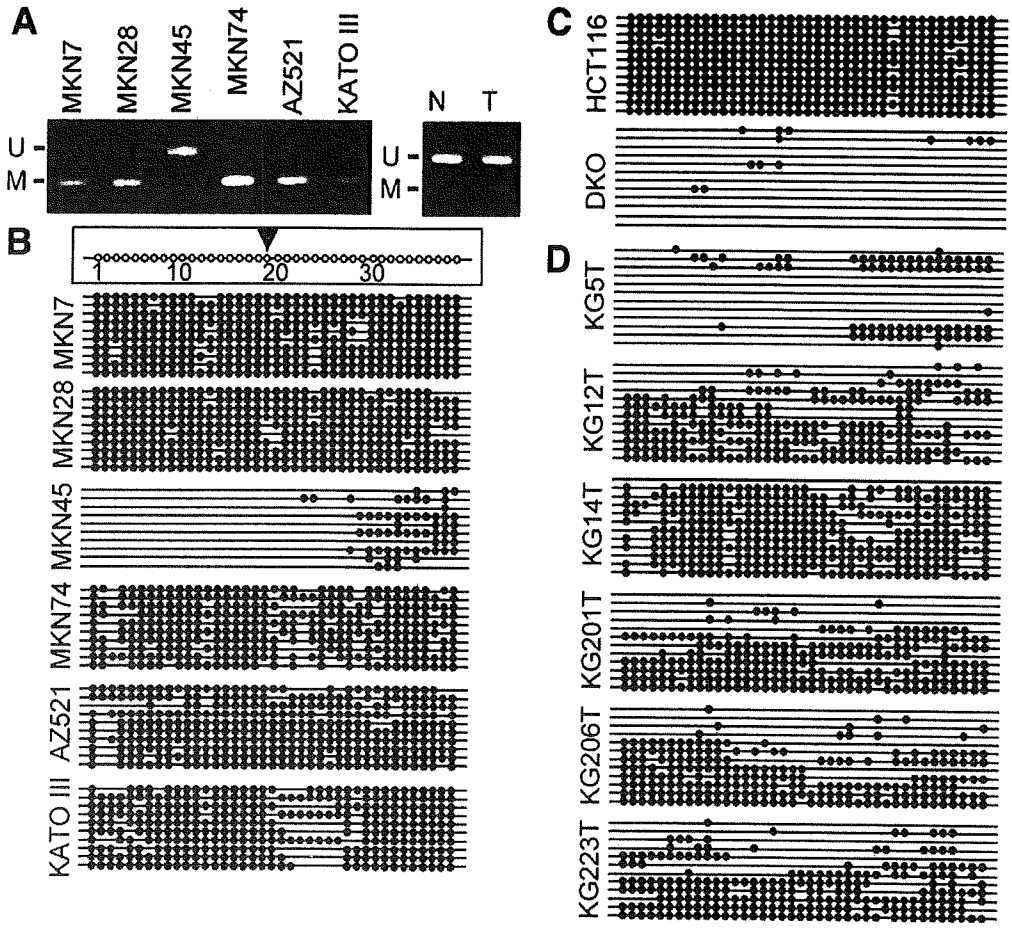

Figure 4. Methylation of the *B4GALNT2* gene in gastric cancer cells and primary gastric carcinomas. (*A*) Combined bisulfite restriction analysis (COBRA) of human gastric cancer cell lines (*left*) and representative results for a primary gastric carcinoma (*right*). M, methylated alleles; N, gastric normal mucosa adjacent to the tumor; T, gastric tumor; U, unmethylated alleles. (*B*, *C* and *D*) Methylation status of individual CpG residues in the *B4GALNT2* gene in human gastric cancer cell lines (*B*), human CRC cell line HCT116 and DKO cells (*C*), and primary gastric carcinomas (*D*) assessed by bisulfite sequencing. Bisulfite-PCR products cloned into the pCR4-TOPO vector were randomly picked up for sequencing. As illustrated in the box at the top of *B*, the line indicates an independent clone of bisulfite-PCR products; it contains 39 consecutive CpGs (*open circles*). For sequencing of the bisulfite–PCR product, the DNA fragment was purified and cloned into the pCR4-TOPO vector (Invitrogen). The start site of translation is indicated by the *arrowhead*. In the results shown below this box, the *filled circles* on the lines for each clone appear only when CpGs are methylated. Cell lines and case ID of tumors are shown at the left in *B* and *C*, respectively.

DNMT3b DKO cells. As expected, methylated CpGs were hardly seen in DKO cells, whereas most of the CpGs examined were methylated in the parental HCT116 cells (Figure 4*C*). Furthermore, it was clearly evident that the upstream of the *B4GALNT2* gene was frequently hypermethylated in human gastric cancer tissues (Figure 4*D*). Sample KG5T, methylation negative by COBRA, and MKN45 cells looked less methylated but included apparently hypermethylated clones. These results imply that DNA hypermethylation in the promoter region of the *B4GALNT2* gene may have contributed to the down-regulation of *B4GALNT2* expression in gastric cancers.

Methylation Status of B4GALNT2 *Gene and Clinicopathologic Characteristics in Primary Gastric Carcinomas*

To understand the significance of hypermethylation in the *B4GALNT2* gene, we analyzed the methylation status of the *B4GALNT2* gene and clinicopathologic characteristics of patients with gastric carcinomas. We deemed that the *B4GALNT2* gene was methylated when the percentage of methylated DNA was 10% by COBRA. Of the 78 primary gastric tumors studied, 39 were classified as methylation positive (Table 1). Univariate analysis revealed no difference between the methylation-positive and -negative groups with respect to age, gender, tumor location, macroscopic type, lymphatic invasion, venous invasion, or pT, pN, or pM status. However, there were significant differences between patients in the methylation-positive and -negative groups with respect to histology (P .012) and EBV status (P .001). EBV was detected in 10 of the 78 tumors, and all EBV-associated tumors were methylation-positive ones. No difference was noted in the frequency of *p53* mutation or the infection of HP between the methylation-positive and -negative groups. To examine the correlation between the

Table 1. Clinicopathologic Features of Gastric Cancer With or Without Methylation of *B4GALNT2*

Characteristics	Total	Number of patients (%)		*P*-value
		Methylated	Unmethylated	
Number of patients	78	39 (50.0)	39 (50.0)	
Mean age SD (*y*)		63.6 13.6	65.4 10.3	.531
Gender				
Male	52 (66.6)	24 (61.5)	28 (71.8)	.472
Female	26 (33.3)	15 (38.5)	11 (28.2)	
Tumor location				
Upper one third	22 (28.2)	14 (35.9)	8 (20.5)	.279
Middle one third	23 (29.5)	9 (23.1)	14 (35.9)	
Lower one third	33 (42.3)	16 (41.0)	17 (43.6)	
Macroscopic type				
0	4 (5.1)	2 (5.1)	2 (5.1)	.98
1	6 (7.7)	3 (7.7)	3 (7.7)	
2	30 (38.5)	14 (35.9)	16 (41.0)	
3	30 (38.5)	15 (38.5)	15 (38.5)	
4	8 (10.3)	5 (12.8)	3 (7.7)	
Histology (Lauren)				
Intestinal	36 (46.2)	12 (30.8)	24 (61.5)	.012
Diffuse	42 (53.8)	27 (69.2)	15 (38.5)	
Lymphatic invasion				
Negative	20 (25.6)	9 (23.1)	11 (28.2)	.78
Positive	58 (74.4)	30 (76.9)	28 (71.8)	
Venous invasion				
Negative	37 (47.4)	20 (51.3)	17 (43.6)	.651
Positive	41 (52.6)	19 (48.7)	22 (56.4)	
Pathologic tumor classification				
pT1	5 (6.4)	3 (7.7)	2 (5.1)	.407
pT2	43 (55.1)	19 (48.7)	24 (61.5)	
pT3	28 (35.9)	15 (38.5)	13 (33.3)	
pT4	2 (2.6)	2 (5.1)	0 (0.0)	
Pathologic lymph node status				
pN0	22 (28.2)	9 (23.1)	13 (33.3)	.373
pN1	28 (35.9)	15 (38.5)	13 (33.3)	
pN2	16 (20.5)	8 (20.5)	8 (20.5)	
pN3	12 (15.4)	7 (17.9)	5 (12.8)	
Pathologic metastasis status				
pM0	66 (84.6)	36 (92.3)	30 (76.9)	.114
pM1	12 (15.4)	3 (7.7)	9 (23.1)	
Stage (pTNM)				
I	18 (23.1)	8 (20.5)	10 (25.6)	.804
II	16 (20.5)	8 (20.5)	8 (20.5)	
III	21 (26.9)	12 (30.8)	9 (23.1)	
IV	23 (29.5)	11 (28.2)	12 (30.8)	
Helicobacter pylori				
Positive	65 (83.3)	33 (84.6)	32 (82.1)	.999
Negative	13 (16.7)	6 (15.4)	7 (17.9)	
Epstein–Barr virus				
Positive	10 (12.8)	10 (25.6)	0 (0.0)	.001
Negative	68 (87.2)	29 (74.4)	39 (100.0)	
p53 mutation				
Positive	19 (24.4)	6 (15.4)	13 (33.3)	.112
Negative	59 (75.6)	33 (84.6)	26 (66.7)	

SD, standard deviation; pTNM, pathologic tumor, lymph node, metastasis status according to the International Union Against Cancer classification system.

Sd^a expression and DNA hypermethylation of *B4GALNT2*, we determined the expression levels of Sd^a carbohydrates in freshly frozen gastric cancers, because Sd^a antigen is expressed as a glycolipid in the stomach; its reactivity to antibodies was lost in formalin-fixed paraffin-embedded samples that we used for our clinicopathologic analysis. Of the 15 freshly frozen gastric cancers studied, the expression of Sd^a determinants was totally lost in all cases as determined by immunohistologic staining; 7 cases were methylation positive by COBRA (data not shown).